Pseudoinverse of the Laplacian and best spreader node in a network

Van Mieghem, P.; Devriendt, K.; Cetinay, H.

DOI
10.1103/PhysRevE.96.032311

Publication date
2017

Document Version
Final published version

Published in
Physical Review E

Pseudoinverse of the Laplacian and best spreader node in a network

P. Van Mieghem,* K. Devriendt,† and H. Cetinay‡
Faculty of EECS, Delft University of Technology, P.O. Box 5031, 2600 GA Delft, The Netherlands
(Received 9 March 2017; published 15 September 2017)

Determining a set of "important" nodes in a network constitutes a basic endeavor in network science. Inspired by electrical flows in a resistor network, we propose the best conducting node j in a graph G as the minimizer of the diagonal element $Q^\dagger_{jj}$ of the pseudoinverse matrix $Q^\dagger$ of the weighted Laplacian matrix of the graph G. We propose a new graph metric that complements the effective graph resistance R_G and that specifies the heterogeneity of the nodal spreading capacity in a graph. Various formulas and bounds for the diagonal element $Q^\dagger_{jj}$ are presented. Finally, we compute the pseudoinverse matrix of the Laplacian of star, path, and cycle graphs and derive an expansion and lower bound of the effective graph resistance R_G based on the complement of the graph G.

DOI: 10.1103/PhysRevE.96.032311

I. INTRODUCTION

We are interested to find the best spreader node in a network and we investigate the pseudoinverse matrix $Q^\dagger$ of the weighted Laplacian $\widetilde{Q}$ of a graph G on N nodes. The major motivation is the appearance of the pseudoinverse $Q^\dagger$ in electrical current flow equations and the relation of $Q^\dagger$ to the effective resistance matrix Ω of the network as reviewed in Sec. II. The overview of known properties of the Laplacian pseudoinverse $Q^\dagger$ in Sec. II illustrates the connection with conservation laws and distance problems. Section III presents new electrical matrix equations, in which the matrix $\widetilde{Q}\Omega$ plays a central role. The symmetric weighted Laplacian $\widetilde{Q}$ and the Laplacian pseudoinverse $Q^\dagger$ have the same orthogonal eigenvector matrix Z, with eigenvectors in its columns. Each such orthogonal matrix Z contains a double set of orthogonal vectors, the column vectors—eigenvectors of $\widetilde{Q}$ and $Q^\dagger$—and the row vectors. This property of orthogonal matrices was called "double orthogonality" and studied in Ref. [1]. The row vectors of Z now possess an interesting property: After scaling by the eigenvalues, they represent N points that form a simplex in $\mathbb{R}^{N-1}$ as explained in Secs. II B and III B. Since the effective resistance matrix Ω can be regarded as a distance matrix, containing the squared distances between those N points, a relation between the volume of that simplex and the number of spanning trees in the graph G is found. We argue that, besides the effective graph resistance R_G, this volume can act as an additional graph metric. Furthermore, we show in Sec. IV that the best electrical spreader node in a graph is the minimizer of the diagonal elements in pseudoinverse matrix $Q^\dagger$. The vector ζ of those diagonal elements in (8) can be regarded as a graph metric vector, further motivated in Sec. V, where we compare the vector ζ in (8) to the betweenness vector, closeness vector, degree vector, and the principal eigenvector of the adjacency matrix. We complement the weighted effective graph resistance $\widetilde{R}_G$, defined in (10), with the upper bound $\blacktriangledown_R$ in (29) of the variance of the components in the vector ζ, that specifies the heterogeneity of the spreading capacity of nodes in a graph. Thus, $\sqrt{\blacktriangledown_R}$ can be regarded as an error bar on the graph metric $\widetilde{R}_G$: a small (large) $\blacktriangledown_R$ increases (decreases) the importance of $\widetilde{R}_G$ as graph specifier. Finally, Appendix B analyzes the diagonal elements of the Laplacian pseudoinverse $Q^\dagger$, Appendix C presents the derivations of the exact pseudoinverse matrix $Q^\dagger$ of the Laplacian matrix of a star, path, and cycle graphs and Appendix D studies the Laplacian and its pseudoinverse of the complement of a graph.

II. BACKGROUND

A. Electrical voltage-current equations in networks

We consider an electrical network, whose topology is specified by a graph G consisting of a set $\mathcal{N}$ of N nodes and a set $\mathcal{L}$ of L weighted links. The link between the nodes i and j possesses a resistance r_{ij}, that results in the link weight $\widetilde{a}_{ij} = 1/r_{ij}$. The weighted symmetric adjacency matrix $\widetilde{A}$ has elements $\widetilde{a}_{ij} = \frac{1}{r_{ij}}$ if a link $(i,j) \in \mathcal{L}$ exists, otherwise $\widetilde{a}_{ij} = 0$. The corresponding weighted symmetric Laplacian

$$\widetilde{Q} = \mathrm{diag}\left(\sum_{k=1}^{N} \widetilde{a}_{ik}\right) - \widetilde{A} \tag{1}$$

with element $\widetilde{q}_{ij} = -\widetilde{a}_{ij}$ if $i \neq j$, else $\widetilde{q}_{ii} = \sum_{k=1}^{N} \widetilde{a}_{ik}$, has zero row and column sum, $\widetilde{Q}u = 0$, where $u = (1,1,\ldots,1)$ is the all-one vector. If each resistance is equal to $r_{ij} = 1$, then the tilde in the matrix notations disappears and we obtain the unweighted adjacency matrix A, the Laplacian Q, where $\sum_{k=1}^{N} a_{ik} = (Au)_i$ reduces to the degree d_i of node i, which is the number of nodes adjacent to i. The $N \times L$ incidence matrix B has, for each link $l = (l_+,l_-) \in \mathcal{L}$, a column with $+1$ on the entry of node l_+ and -1 on the entry of the other node l_-; thus, $B_{l_+,l} = +1$ and $B_{l_-,l} = -1$ so that B has a zero column sum, $u^T B = 0$. The incidence matrix is related [2] to the Laplacian matrix by $Q = BB^T$.

We further define the voltage v_i of node i in the network circuit and the current $y_l = y_{ij}$ through the resistors of link l between node i and j, which is directed so that $y_{ij} = -y_{ji}$. We call x_i the external current injected into node i. The voltages and currents are related by the law of Ohm and the laws of Kirchhoff. Ohm's law $v_a - v_b = r_{ab} y_{ab}$ states that the voltage

*P.F.A.VanMieghem@tudelft.nl
†K.L.T.Devriendt@student.tudelft.nl
‡H.Cetinay-Iyicil@tudelft.nl

difference $v_a - v_b$ over the resistor r_{ab} is proportional to the current y_{ab} through the resistor. Using the incidence matrix B of the network, Ohm's law is written in matrix form as

$$y = \mathrm{diag}\left(\frac{1}{r_l}\right) B^T v, \tag{2}$$

where y is the $L \times 1$ link current vector and v is the $N \times 1$ vector with nodal voltages or potentials and the $L \times L$ diagonal matrix $\mathrm{diag}(\frac{1}{r_l})$, in which r_l is the resistance of link l, contains all L link resistors in the graph G.

Kirchhoff's current law is based on the conservation of electrical charge and current and states that, for any node, the net sum of currents flowing in and out of the node is zero. Considering both the external $N \times 1$ nodal current vector x and the $L \times 1$ link current vector y, the conservation law for a node a is $\sum_{b \in \mathcal{N}(a)} y_{ab} = x_a$, where $\mathcal{N}(a)$ is the set of all neighbors of node a. Using the incidence matrix B, leads to the matrix equation

$$x = By, \tag{3}$$

from which the basic conservation law for currents entering and leaving the network follows as

$$u^T x = 0 \tag{4}$$

after multiplying both sides in (3) with u^T and invoking the characteristic property $u^T B = 0$ of the incidence matrix B. Substituting (2) into (3) yields $x = B\mathrm{diag}(\frac{1}{r_l})B^T v$. Alternatively, we combine Kirchhoff's current law $\sum_{k=1}^{N} a_{ik} y_{ik} = x_i$ with Ohm's law $v_i - v_k = r_{ik} y_{ik}$,

$$x_i = \sum_{k=1}^{N} \frac{a_{ik}}{r_{ik}}(v_i - v_k) = v_i \sum_{k=1}^{N} \widetilde{a}_{ik} - \sum_{k=1}^{N} \widetilde{a}_{ik} v_k,$$

which is written in matrix form as

$$x = \left(\mathrm{diag}\left(\sum_{k=1}^{N} \widetilde{a}_{ik}\right) - \widetilde{A}\right) v.$$

With the definition (1) of the weighed Laplacian $\widetilde{Q}$, we obtain[1]

$$x = \widetilde{Q} v, \tag{5}$$

illustrating that the graph's weighted Laplacian matrix $\widetilde{Q}$ transforms nodal voltages to injected currents in nodes. In addition, we find the weighted companion of the Laplacian relation $Q = BB^T$,

$$\widetilde{Q} = B\mathrm{diag}\left(\frac{1}{r_l}\right) B^T.$$

The inversion of the fundamental current-voltage relation $x = \widetilde{Q} v$ in (5) between the $N \times 1$ injected current flow vector x into nodes of the network and the $N \times 1$ voltage vector v at the nodes is complicated by the fact that $\det \widetilde{Q} = 0$, which follows from the characteristic property $\widetilde{Q} u = 0$ of the weighted Laplacian. Although the inverse weighted Laplacian matrix $\widetilde{Q}^{-1}$ does not exist, the current-voltage inversion problem can be shown to be $v = Q^\dagger x + \frac{u^T v}{N} u$, where $Q^\dagger$ is the pseudoinverse of the weighted Laplacian $\widetilde{Q}$, obeying $\widetilde{Q} Q^\dagger = Q^\dagger \widetilde{Q} = I - \frac{1}{N} J$ with the all-one matrix $J = uu^T$, and where the average voltage in the network equals $v_{\mathrm{av}} = \frac{u^T v}{N}$. By choosing $v_{\mathrm{av}} = 0$ as the reference potential, the inverse of $x = \widetilde{Q} v$ takes the elegant form of

$$v = Q^\dagger x, \tag{6}$$

which is close to the usual matrix inversion. If the graph G is unweighted, then $\widetilde{Q}$ reduces to the Laplacian Q of G and $Q^\dagger$ to the pseudoinverse $\widehat{Q}^{-1}$ of the Laplacian Q.

From the voltage-current relation (6), the effective resistance matrix Ω can be derived [2,3] as

$$\Omega = \zeta u^T + u \zeta^T - 2Q^\dagger, \tag{7}$$

where the vector

$$\zeta = (Q^\dagger_{11}, Q^\dagger_{22}, \ldots, Q^\dagger_{NN}) \tag{8}$$

contains the diagonal elements of the pseudoinverse matrix $Q^\dagger$ of the weighted Laplacian $\widetilde{Q}$ in (1). In particular, the effective resistance between node a and b equals

$$\omega_{ab} = (e_a - e_b)^T Q^\dagger (e_a - e_b) = Q^\dagger_{aa} + Q^\dagger_{bb} - 2Q^\dagger_{ab}, \tag{9}$$

where e_k is the basic vector with the mth component equal to $(e_k)_m = \delta_{mk}$ and δ_{mk} is the Kronecker-delta: $\delta_{mk} = 1$ if $m = k$; otherwise, $\delta_{mk} = 0$. The weighted effective graph resistance $\widetilde{R}_G$ is defined as the sum of the effective resistances between all possible pairs of nodes in the graph G,

$$\widetilde{R}_G = \sum_{i=1}^{N} \sum_{j=i+1}^{N} \omega_{ij} = \frac{1}{2} u^T \Omega u. \tag{10}$$

B. Spectral analysis of the weighted Laplacian $\widetilde{Q}$ and its pseudoinverse $Q^\dagger$

If $\widetilde{Q} = \sum_{k=1}^{N-1} \widetilde{\mu}_k \widetilde{z}_k \widetilde{z}_k^T$ is the spectral decomposition of the weighted Laplacian $\widetilde{Q}$, where the normalized eigenvector $\widetilde{z}_k$ belongs to the k-largest eigenvalue $\widetilde{\mu}_k$ (thus $\widetilde{\mu}_1 \geqslant \ldots \geqslant \widetilde{\mu}_{N-1} > \widetilde{\mu}_N = 0$ implying that the graph G is assumed to be connected), then the pseudoinverse $Q^\dagger$ of the weighted Laplacian $\widetilde{Q}$ is defined as

$$Q^\dagger = \sum_{k=1}^{N-1} \widetilde{\mu}_k^{-1} \widetilde{z}_k \widetilde{z}_k^T. \tag{11}$$

In general, the pseudoinverse $Q^\dagger$ is not a weighted Laplacian, because the off-diagonal elements of $Q^\dagger$ can be positive contradicting the definition (1) of the weighed Laplacian $\widetilde{Q}$. Both $N \times N$ matrices $\widetilde{Q}$ and $Q^\dagger$ are symmetric and share the same set of eigenvectors $\widetilde{z}_1, \widetilde{z}_2, \ldots, \widetilde{z}_{N-1}$, normalized and obeying $\widetilde{z}_m^T \widetilde{z}_k = \delta_{mk}$, that are all orthogonal to the all-one vector $u = \sqrt{N} \widetilde{z}_N$, which is the eigenvector of any Laplacian matrix corresponding to the eigenvalue $\widetilde{\mu}_N = 0$. Hence, we have that both $\widetilde{Q} u = 0$ and $Q^\dagger u = 0$, which implies that the set of $N - 1$ orthogonal $N \times 1$ vectors $\widetilde{z}_1, \widetilde{z}_2, \ldots, \widetilde{z}_{N-1}$ (without $\widetilde{z}_N = \frac{u}{\sqrt{N}}$) is insufficient to span the N-dimensional space but

[1] Although the current-voltage relation (5) has been derived for resistances only, the analysis is readily generalized to $x(s) = \widetilde{Q}(s) v(s)$ for inductive and capacitive passive elements with link impedance $r_l + sL_l + \frac{1}{s} C_l$, after a Laplace transform of the electrical differential equations in time t to the s domain.

only the space of all vectors that are orthogonal to the all-one vector $u = \sqrt{N}\widetilde{z}_N$. Thus, from $Q^\dagger \widetilde{Q} = I - \frac{1}{N}J$ and $Q^\dagger u = 0$, we can write

$$Q^\dagger(\widetilde{Q} + \alpha uu^T) = I - \frac{1}{N}J,$$

where $\widetilde{Q} + \alpha uu^T$ with $J = uu^T$ has full rank [i.e., $\det(\widetilde{Q} + \alpha J) \neq 0$], provided $\alpha \neq \mu_N = 0$. Hence, for any nonzero number α, an alternative representation for the Laplacian pseudoinverse $Q^\dagger$ follows [2, p. 205] as[2]

$$Q^\dagger = (\widetilde{Q} + \alpha J)^{-1}\left(I - \frac{1}{N}J\right). \tag{12}$$

Combining the definition (10) of the effective graph resistance R_G with that of Ω in (7) and the spectral decomposition (11) shows that

$$\widetilde{R}_G = N \operatorname{tr}(Q^\dagger) = N \sum_{k=1}^{N-1} \widetilde{\mu}_k^{-1}. \tag{13}$$

The effective graph resistance $\widetilde{R}_G$ (of a weighted graph) is a graph metric [4] that reflects the overall transport capability of the graph G: The lower $\widetilde{R}_G$, the better the graph conducts traffic. The effective graph resistance is related, as shown in (13), to the eigenvalues of the Laplacian matrix [4], but also to uniform spanning trees [5], random walks [6], and the betweenness centrality [7]. Often, the effective graph resistance R_G appears as a robustness metric for power grids [8–10]. The effect of the removal of links on R_G is analyzed in Ref. [11], and several bounds on R_G are deduced. A new, tighter lower bound (B12) for R_G is derived in Appendix B. The Laplacian pseudoinverse $\widehat{Q}^{-1}$ of the connected complement G^c of a connected graph G, together with the effective graph resistance R_{G^c} (and bounds) are studied in Appendix D.

Let Z denote the $N \times N$ orthogonal matrix with the eigenvectors $\widetilde{z}_1, \widetilde{z}_2, \ldots, \widetilde{z}_N$ in the columns and $M = \operatorname{diag}(\widetilde{\mu}_1, \widetilde{\mu}_2, \ldots, \widetilde{\mu}_N)$, and then the spectral decomposition of the weighted Laplacian $\widetilde{Q}$ and its pseudoinverse $Q^\dagger$ is $\widetilde{Q} = ZMZ^T$ and $Q^\dagger = ZM^\dagger Z^T$, where $M^\dagger = \operatorname{diag}(\frac{1}{\widetilde{\mu}_1}, \frac{1}{\widetilde{\mu}_2}, \ldots, 0)$. Since the Laplacian eigenvalues are non-negative, we have that $M = M^{1/2}M^{1/2}$ and similarly for $M^\dagger$, so that

$$\widetilde{Q} = ZM^{1/2}M^{1/2}Z^T = Z\sqrt{M}(Z\sqrt{M})^T$$

and

$$Q^\dagger = Z\sqrt{M^\dagger}(Z\sqrt{M^\dagger})^T.$$

If we define the $N \times N$ matrix $S = (Z\sqrt{M})^T$ and $S^\dagger = (Z\sqrt{M^\dagger})^T$, then S and $S^\dagger$ contain as columns the scaled row vectors of Z. The column vectors of Z are the eigenvectors of $\widetilde{Q}$ (and $Q^\dagger$). The row vectors of Z also form an orthogonal set of vectors spanning the N-dimensional space. Earlier [1, Appendix], we have called this fundamental property "double orthogonality" that follows from the fact that any orthogonal matrix X satisfies $X^TX = XX^T = I$. Due to the zero last row in S and $S^\dagger$, their column vectors do not span the N-dimensional space, but only the subspace of $\mathbb{R}^N$ orthogonal to the all-one vector u. Hence, the weighted Laplacian $\widetilde{Q} = S^TS$ and its corresponding pseudoinverse $Q^\dagger = S^{\dagger T}S^\dagger$ are Gram matrices (see, e.g., Refs. [12, Sec. 8.7], [2, p. 241], [13], as well as Fiedler's geometric interpretation [14]). In particular, the diagonal element $(Q^\dagger)_{jj} = \sum_{k=1}^{N-1}(s_j^\dagger)_k^2 = \|s_j^\dagger\|_2^2$ expresses the Euclidean distance of the node j in $\mathbb{R}^{N-1}$, because the vector $s_j^\dagger = (\frac{(\widetilde{z}_1)_j}{\sqrt{\widetilde{\mu}_1}}, \frac{(\widetilde{z}_2)_j}{\sqrt{\widetilde{\mu}_2}}, \ldots, \frac{(\widetilde{z}_{N-1})_j}{\sqrt{\widetilde{\mu}_{N-1}}}, 0)^T \in \mathbb{R}^{N-1}$, featuring $(s_j^\dagger)^T s_m^\dagger = \sum_{k=1}^{N-1}(s_j^\dagger)_k(s_m^\dagger)_k = \sum_{k=1}^{N-1}\frac{(\widetilde{z}_k)_j}{\sqrt{\widetilde{\mu}_k}}\frac{(\widetilde{z}_k)_m}{\sqrt{\widetilde{\mu}_k}} = (Q^\dagger)_{jm}$. Thus, the set $(s_1^\dagger, s_2^\dagger, \ldots, s_N^\dagger)$ of N column vectors of $S^\dagger$ are linearly dependent because $s_j^\dagger \in \mathbb{R}^{N-1}$ (due to the last zero vector component); they are not orthogonal and their scalar products or projections on each other, $(s_j^\dagger)^T s_m^\dagger = (Q^\dagger)_{jm}$, return the elements of the pseudoinverse matrix $Q^\dagger$. Furthermore, the distance between two nodes j and m with coordinates $s_j^\dagger$ and $s_m^\dagger$ in $\mathbb{R}^{N-1}$, respectively, is

$$\begin{aligned}\|s_j^\dagger - s_m^\dagger\|_2^2 &= (s_j^\dagger - s_m^\dagger)^T(s_j^\dagger - s_m^\dagger)\\ &= (Q^\dagger)_{jj} + (Q^\dagger)_{mm} - 2(Q^\dagger)_{jm} = \omega_{jm}\end{aligned}$$

and equal to the effective resistance ω_{jm} in (9) between the nodes j and m in the weighted graph. Hence, the elements of the effective resistance matrix Ω are squared distances between two nodes in the N-dimensional $s^\dagger$ basis. Based on this distance notion, Ranjan and Zhang [15] have proposed to consider $\frac{1}{(Q^\dagger)_{jj}}$ as the topological centrality of node j: The closer node j is to the origin in the $s^\dagger$ space, the higher its topological centrality or importance.

C. Extension

While the weighted Laplacian $\widetilde{Q}$ and its pseudoinverse $Q^\dagger$ were approached so far from an electrical point of view, their applicability is far wider. First, a weighted Laplacian $\widetilde{Q}$ describes many processes that are "linear" in or proportional to the network topology when ignoring friction, e.g., in water flow networks, mechanical systems such as a spring-mass network, gas networks, and warmth diffusion in networks. The process equivalence between those systems is illustrated in Table I.

Second, any infinitesimal generator of a continuous-time Markov process is minus a weighted Laplacian $\widetilde{Q}$ as mentioned in Ref. [16, p. 207], where the nodes in the Markov graph represent the states of the Markov process and the link

TABLE I. Equivalence between linear systems.

Electrical circuit	Voltage	Current
Hydraulic circuit	Pressure (height of liquid)	Volume flow
Mechanical system	Force	Displacement velocity
Thermal system	Temperature	Heat flow
...	...	...

[2]For example, the pseudoinverse of the Laplacian $Q_{K_N} = NI - J$ of the complete graph K_N follows from (12) after choosing $\alpha = 1$ as $(\widehat{Q}^{-1})_{K_N} = \frac{1}{N}Q_{K_N}$.

weights are the transition rates between the states. In most cases, however, the infinitesimal generator is not symmetric. Furthermore, any stochastic process can be approximated arbitrarily close by a continuous-time Markov chain provided the state space (i.e., the number of states in the Markov chain) is sufficiently large. While the unweighted Laplacian Q (without tilde) specifies a property of the graph's topology, the weighted version $\widetilde{Q}$ (with tilde and often the infinitesimal generator has a much larger dimension than N, see, e.g., a Markovian epidemic process [17,18] whose state space is 2^N) can characterize approximately any dynamic process on the graph. The stochastic connection explains why random walks, which are relatively simple continuous-time Markov processes on a graph, and the effective resistances are related [4,13,19]. A random walk on the weighted graph G is a stochastic process in which a random walker at node i has probability $P_{ij} = \frac{\widetilde{a}_{ij}}{\sum_{k=1}^{N} \widetilde{a}_{ki}}$ to visit node j in the next time step. This discrete-time transition probability matrix P can also be written in terms of the weighted adjacency matrix $\widetilde{A}$ of G as $P = \{\mathrm{diag}[(\widetilde{A}u)_i]\}^{-1}\widetilde{A}$. Such random walks naturally appear in Markov processes, where the discrete-time transition probability matrix relates to the continuous-time infinitesimal generator in the same way as the random-walk transition probability matrix P relates to the weighted Laplacian $\widetilde{Q}$. The expected hitting time H_{ij} equals the expected number of steps of a random walker that starts at node i and stops at node j. The commute time, defined as $C_{ij} = H_{ij} + H_{ji}$, is then the expected number of steps of a random walker that starts at node i, arrives at j, and returns to i and conversely since $C_{ij} = C_{ji}$. The connection between commute time and effective resistance is given [19] by $C_{ij} = 2\widetilde{L}\omega_{ij}$ or, in matrix notation, $C = 2\widetilde{L}\Omega$, where $\widetilde{L} = \frac{1}{2}u^T\widetilde{A}u$ is the sum of all the link weights or simply the number L of links in an unweighted graph.

Finally, the continuous companion of the weighted Laplacian is the Laplacian operator, whose inverse is related to the Green operator and Green's functions, for which we refer to Refs. [20,21]. Using Green's functions, Chung and Yau [20] solve $x = Qv$ for the vector x and the Green's function $\mathcal{G}$ in their analysis equals the pseudoinverse $Q^\dagger$.

III. NEW ELECTRICAL MATRIX EQUATIONS

From the definition (9) of the effective resistance, we present an alternative expression that describes the $N \times 1$ external current vector x and the $N \times 1$ voltage vector v in terms of the effective resistance matrix Ω in (7). All theorems in this section are proved in Appendix A.

Theorem 1. In an electrical circuit on N nodes with effective resistance matrix Ω, the external current x injected in each node induces the nodal voltages,

$$v = -\frac{1}{2N} Q_{K_N} \Omega x, \tag{14}$$

where $Q_{K_N} = NI - J$ is the Laplacian of the complete graph K_N on N nodes.

Since $u^T Q_{K_N} = 0$, we observe from (14) that $u^T v = 0$ and $v_{\mathrm{av}} = 0$, which is our choice of voltage reference. Theorem 1 and the external current-voltage relation (6) lead to

Theorem 2. For a weighted Laplacian matrix $\widetilde{Q}$ with corresponding effective resistance matrix Ω, the matrix $-\frac{1}{2}\widetilde{Q}\Omega$ behaves like an identity matrix for right-multiplication of vectors orthogonal to the all-one vector u. In other words, for any vector x such that $u^T x = 0$, we can write

$$x = -\tfrac{1}{2}\widetilde{Q}\Omega x. \tag{15}$$

The "voltage v versus external current x " vector relation $v = -\frac{1}{2N} Q_{K_N}\Omega x$ in (14) and $v = Q^\dagger x$ in (6) are complementary: For any current vector x obeying $x^T u = 0$, it holds that

$$Q^\dagger x = -\frac{1}{2N} Q_{K_N}\Omega x, \tag{16}$$

representing a computational method for the Laplacian pseudoinverse $Q^\dagger$ when the effective resistance matrix Ω is known or when Ω is more easily obtained than the Laplacian pseudoinverse $Q^\dagger$ (as illustrated for the path graph in Appendix C 2 b).

A. Power-based definition of effective graph resistance

By forcing a current I_c between a pair of nodes a and b and measuring the voltage difference $v_{ab} = v_a - v_b$, the effective resistance follows as $\omega_{ab} = v_{ab}/I_c$, while a power $\mathcal{P} = v_{ab} I_c = I_c^2 \omega_{ab}$ is dissipated in the network (and thus drained from the external source). We thus observe that the effective resistance ω_{ab} between a pair of nodes a and b can also be measured as the total dissipated power $\mathcal{P} = I_c^2\omega_{ab}$ in the network for a unit external current $I_c = 1$ A forced between the nodes a and b. In general, the total dissipated power equals

$$\mathcal{P} = x^T v$$

and introducing the inverse relations $x = \widetilde{Q}v$ and $v = Q^\dagger x$ yields

$$\mathcal{P} = v^T\widetilde{Q}v = x^T Q^\dagger x. \tag{17}$$

For any external current vector obeying $x^T u = 0$, it follows from the definition (7) of the effective resistance matrix Ω that

$$x^T\Omega x = -2x^T Q^\dagger x. \tag{18}$$

Hence, we arrive at the quadratic form for the power dissipation in the network[3]

$$\mathcal{P} = -\tfrac{1}{2}x^T\Omega x.$$

For the specific external current vector $x = I_c(e_a - e_b)$, we obtain again with (A2)

$$\mathcal{P} = -\tfrac{1}{2}x^T\Omega x = -\tfrac{1}{2}I_c^2(e_a - e_b)^T\Omega(e_a - e_b) = I_c^2\omega_{ab}. \tag{19}$$

We conclude that forcing a unit current $I_c = 1$ A between a pair of nodes a and b results in two different ways to determine the effective resistance ω_{ab}: one via the total power (19) dissipated and the other via the local voltage difference (A1).

[3]Repeated introductions of (15) yields, for any integer $n \geqslant 0$,

$$\mathcal{P} = \frac{(-1)^{n+1}}{2^{n+1}} x^T\Omega(\widetilde{Q}\Omega)^n x.$$

Ghosh *et al.* [13] give a stochastic interpretation of the effective graph resistance R_G. Injecting a random external current p in a network G, satisfying $u^T p = 0$, with expectation $E[p] = 0$ and covariance matrix $E[pp^T] = I - J/N$ results in an expected dissipated power of $E[\mathcal{P}] = \frac{1}{N}\widetilde{R}_G$. Indeed, taking the expectation of the power in (17), we compute

$$E[\mathcal{P}] = E[p^T Q^\dagger p] = E\left[\sum_{i=1}^{N}\sum_{j=1}^{N} Q^\dagger_{ij} p_i p_j\right]$$
$$= \sum_{i=1}^{N}\sum_{j=1}^{N} Q^\dagger_{ij} E[p_i p_j] = \mathrm{trace}(Q^\dagger E[pp^T]).$$

Introducing the projector orthogonal to the u vector, $E[pp^T] = I - J/N$ yields $Q^\dagger E[pp^T] = Q^\dagger$ and, with (13), we arrive at $E[\mathcal{P}] = \frac{1}{N}\widetilde{R}_G$. For a random vector X, the covariance matrix $\Sigma_X = E[XX^T] - E[X](E[X])^T$ of the form $\Sigma_X = I - J/N$ indicates that $\mathrm{Cov}[X_i, X_j] = -\frac{1}{N}$ between each vector component is equal. Such random vectors can be constructed from a Gaussian vector with independent components [16, p. 75]. The observation of Ghosh *et al.* [13] is peculiar, because we can show that $E[\mathcal{P}] = \frac{1}{N}\widetilde{R}_G$ only holds for the particular covariance matrix $\Sigma_X = I - \alpha J/N$ where $\alpha = 1$.

B. The matrix $\widetilde{Q}\Omega$ and the geometrical interpretation of Ω

With the definition (7) of Ω, we have $\widetilde{Q}\Omega = \widetilde{Q}\zeta u^T + \widetilde{Q}u\zeta^T - 2\widetilde{Q}Q^\dagger$ and thus

$$\widetilde{Q}\Omega = \widetilde{Q}\zeta u^T - 2\left(I - \frac{1}{N}J\right), \tag{20}$$

which again leads to (15) for any vector x orthogonal to u.

All columns in the matrix $\widetilde{Q}\zeta u^T$ are the same and equal to the vector $\widetilde{Q}\zeta$ and $\widetilde{Q}\Omega u = N\,\widetilde{Q}\zeta$, so that the vector $\widetilde{Q}\zeta = \frac{1}{N}\widetilde{Q}\Omega u$, with mth component $(\widetilde{Q}\zeta)_m = \sum_{k=1}^{N}\widetilde{q}_{mk}Q^\dagger_{kk}$, equals the average row sum of the matrix $\widetilde{Q}\Omega$. After taking the transpose and invoking the symmetry of Ω and $\widetilde{Q}$, the matrix equation

$$\Omega\widetilde{Q} = u(\widetilde{Q}\zeta)^T - 2\left(I - \frac{1}{N}J\right)$$

indicates that

$$\widetilde{Q}\Omega - \Omega\widetilde{Q} = \widetilde{Q}\zeta u^T - u(\widetilde{Q}\zeta)^T,$$

implying that $\widetilde{Q}\Omega$ and $\Omega\widetilde{Q}$ do not commute (unless the vector $\widetilde{Q}\zeta = 0$ as in the complete graph K_N) and that eigenvectors of Ω and $\widetilde{Q}$ are generally different [2, p. 253]. Moreover, $\Omega\widetilde{Q}u = u(\widetilde{Q}\zeta)^T u = 0$ indicates that $(\widetilde{Q}\zeta)^T u = 0$ or that the sum of the elements of the vector $\widetilde{Q}\zeta$ is zero.

Equation (15) in Theorem 2, $\widetilde{Q}\Omega x = -2x$, is an eigenvalue equation: Each external nodal current vector, satisfying $u^T x = 0$, is an eigenvector of the matrix $\widetilde{Q}\Omega$ belonging to the eigenvalue -2. The eigenvalues of the $N \times N$ asymmetric matrix $\widetilde{Q}\Omega$ in (20) are the zeros in λ of the characteristic polynomial,

$$c_{\widetilde{Q}\Omega}(\lambda) = \det(\widetilde{Q}\Omega - \lambda I),$$

which is with (20) and $J = uu^T$

$$c_{\widetilde{Q}\Omega}(\lambda) = \det\left[\left(\widetilde{Q}\zeta + \frac{2}{N}u\right)u^T - (\lambda + 2)I\right].$$

Invoking the "rank one update" formula [2, p. 256], $\det(I + cd^T) = 1 + d^T c$, yields

$$c_{\widetilde{Q}\Omega}(\lambda) = (-1)^N\lambda(\lambda + 2)^{N-1}.$$

Hence, the matrix $\widetilde{Q}\Omega$ has $N - 1$ eigenvalues equal to $\lambda = -2$, belonging to each possible external current x orthogonal to u, and one zero eigenvalue that must be a linear combination[4] of the eigenvector u and x. Hence,

$$\widetilde{Q}\Omega(au + bx) = aN\widetilde{Q}\zeta - 2bx = 0$$

so that $x = \frac{aN}{2b}\widetilde{Q}\zeta$ and the eigenvector belonging to $\lambda = 0$ equals $u + \frac{N}{2}\widetilde{Q}\zeta$.

From the matrix relation (20), we find $-\frac{1}{2}\widetilde{Q}\Omega\widetilde{Q} = \widetilde{Q}$, which suggests that we consider $-\frac{1}{2}\Omega$ as a generalized inverse of the Laplacian $\widetilde{Q}$. Fiedler [22] points to a more elegant approach in presenting a remarkable inverse block matrix relation, from which we deduce

$$-\frac{1}{2}\begin{bmatrix}0 & u^T\\ u & \Omega\end{bmatrix} = \begin{bmatrix}\zeta^T\widetilde{Q}\zeta + \frac{4R_G}{N^2} & -\left(\widetilde{Q}\zeta + \frac{2}{N}u\right)^T\\ -\left(\widetilde{Q}\zeta + \frac{2}{N}u\right) & \widetilde{Q}\end{bmatrix}^{-1}. \tag{21}$$

Relation (21) can be verified from the general inverse formula for block matrices [23, p. 123]. In the block matrix at the right-hand side of (21) appears the eigenvector $\widetilde{Q}\zeta + \frac{2}{N}u$ of the matrix $\widetilde{Q}\Omega$ belonging to the zero eigenvalue.[5] Equation (21) is particularly interesting for at least two reasons.

First, the block matrix relation (21) transforms the *function* in a network via measurements or observations resulting in the Ω matrix (left-hand side) to the *structure* of the network (right-hand side), specified by $\widetilde{Q}$ in (1). Especially in networks, such as the human brain, whose internal topology is opaque and only at special places outside the skull can be measured, the new block matrix relation (21) may shed new light on the relation between the functional brain (left-hand side) to the anatomical brain (right-hand side), whose study is timely (see, e.g., Refs. [25,26]).

Second, the block matrix relation (21) reveals a geometric interpretation of the Ω matrix. Recall from Sec. II that by the Gram equivalent $Q^\dagger = S^{\dagger T}S^\dagger$, where $S^\dagger = (Z\sqrt{M^\dagger})^T$, we found that $\omega_{ij} = ||s^\dagger_i - s^\dagger_j||_2^2$. Although the orthogonal eigenvector matrix Z includes the normalized all-one vector $\frac{u}{\sqrt{N}}$ belonging to the zero eigenvalue $\widetilde{\mu}_N = 0$ in the Nth column, the corresponding Nth row in $S^\dagger$ is the null vector, which we can exclude, so that the matrix $S^\dagger$ effectively has

[4] Since $\widetilde{Q}\Omega$ is not symmetric, the eigenvectors are not necessarily orthogonal but independent.

[5] We can geometrically interpret the term $\zeta^T\widetilde{Q}\zeta + \frac{4R_G}{N^2}$. If R is the radius of the circumsphere of the simplex, defined by the Gram matrix $S^\dagger$ of the pseudoinverse Laplacian, then the relation $R^2 = \zeta^T\widetilde{Q}\zeta + \frac{4R_G}{N^2}$ holds. The circumsphere of the simplex was first described by Coxeter [24] in 1930.

the dimensions $(N-1)\times N$. Thus, the ith column vector $s_i^\dagger$ in $S^\dagger$ can represent a point p_i in the $N-1$-dimensional space with coordinates $s_i^\dagger \in \mathbb{R}^{N-1}$ and $\omega_{ij} = ||s_i^\dagger - s_j^\dagger||_2^2$ is the squared Euclidean distance between the points p_i and p_j. In the field of distance geometry, the determinant $\det\left[\begin{smallmatrix}0 & u^T\\ u & H\end{smallmatrix}\right]$, where H is an $N\times N$ matrix with squared Euclidean distances between a set of N points in $\mathbb{R}^{N-1}$, is called the Cayley-Menger determinant and introduced by Menger [27]. For a consistent distance matrix H, the Cayley-Menger determinant is related [27] to the volume V of the convex hull of the N points (also called the simplex of those points) by

$$V^2 = \frac{(-1)^N}{2^{N-1}((N-1)!)^2}\det\begin{bmatrix}0 & u^T\\ u & H\end{bmatrix}. \tag{22}$$

The effective resistance matrix Ω obeys the characteristics of a distance matrix H that corresponds [22] to a hyperacute simplex of N points in $\mathbb{R}^{N-1}$ with squared distance matrix $H=\Omega$, which means that all $(N-2)$-dimensional faces have interior angles that are acute or right. In particular, Sharpe [28] shows that problems on resistive networks are equivalent to geometric problems on acute-angled simplices imbedded in a multidimensional Euclidean space.

Now, if we call $T_i \subset \mathcal{L}$ the link set of a specific spanning tree, then $\prod_{\forall l\in T_i} w_l$ is the product of all the link weights w_l of that specific tree T_i. The number of weighted spanning trees then equals

$$\tilde{\xi} = \sum_{\forall T_i}\prod_{\forall l\in T_i} w_l. \tag{23}$$

Interestingly, this number $\tilde{\xi}$ of weighted spanning trees can also be expressed [2, p. 77] in terms of the Laplacian eigenvalues as

$$\tilde{\xi} = \frac{1}{N}\prod_{k=1}^{N-1}\widetilde{\mu}_k.$$

Combining the block matrix relation (21) and the relation between minors of the Laplacian and the number of spanning trees (i.e., the matrix-tree theorem [2, p. 75]), we can express the Cayley-Menger determinant of Ω in terms of the *number of weighted spanning trees*.

Theorem 3. Consider a graph G with weighted Laplacian matrix $\widetilde{Q}$, effective resistance matrix Ω, and the number $\tilde{\xi}$ of weighted spanning trees. The volume V_G of the simplex formed by N points $p_i \in \mathbb{R}^{N-1}$, with the columns of $\sqrt{M^\dagger}Z^T$ (but excluding the Nth row in Z^T) as coordinates, is given by

$$V_G = \frac{1}{(N-1)!\sqrt{\tilde{\xi}}}. \tag{24}$$

The main interest of Theorem 3 lies in the connection with the effective graph resistance $\widetilde{R}_G$. If "$\propto$" denotes proportionality in

$$\widetilde{R}_G = N\sum_{k=1}^{N-1}\widetilde{\mu}_k^{-1} \propto \sum_{k=1}^{N-1}\frac{1}{\widetilde{\mu}_k}, \tag{25}$$

$$V_G = \frac{\sqrt{N}}{(N-1)!\sqrt{\prod_{k=1}^{N-1}\widetilde{\mu}_k}} \propto \sqrt{\prod_{k=1}^{N-1}\frac{1}{\widetilde{\mu}_k}}, \tag{26}$$

then (25) illustrates that the effective graph resistance $\widetilde{R}_G$ is proportional to the arithmetic mean of the inverse Laplacian eigenvalues, while (26) shows that the simplex volume V_G is related to the geometric mean of the inverse Laplacian eigenvalues.[6] As a result, the simplex volume V_G and the effective graph resistance $\widetilde{R}_G$ capture "similar information" in the sense that both represent a mean of the inverse Laplacian eigenvalues and "complementary information" in that for different graphs with the same effective graph resistance $\widetilde{R}_G$, the simplex volume V_G will differ and thus allows us to discriminate between these graphs. Moreover, for a fixed arithmetic mean, the geometric mean represents the spread of the elements around the mean, for certain notions of "spread" [29]. Finally, the harmonic, geometric and arithmetic mean inequality (D2)

$$\frac{N-1}{2\widetilde{L}} \leqslant \sqrt[N-1]{\frac{((N-1)!)^2}{N}V_G^2} \leqslant \frac{\widetilde{R}_G}{(N-1)N},$$

where $\widetilde{L} = \frac{1}{2}u^T\widetilde{A}u$ is the sum of the link weights in the graph G, indicates that an increase in the simplex volume V_G cannot lead to a decrease in the effective graph resistance $\widetilde{R}_G$. Alternatively, less (weighted) spanning trees $\tilde{\xi}$, equivalent by (24) to a larger volume V_G of the simplex in $\mathbb{R}^{N-1}$, complicate currents to flow over the network, resulting in higher effective resistances and, thus, a higher $\widetilde{R}_G$.

IV. THE BEST ELECTRICAL SPREADER NODE

We define the node k^*, that is electrically best connected to all other nodes, as the minimizer over all nodes $j\in G$ of $(\Omega u)_j = \sum_{i=1}^N \omega_{ij}$, which is the sum of the effective resistances between node j and any other node i in the graph G. In other words, if a current I_c is injected in node k^* and all other nodes in G are sinks, then the potential of node k^* is the lowest among all nodes. Hence, we may consider $(\Omega u)_j$ as a graph centrality metric, in addition to eigenvector centrality metrics [1], that reflects how good node j spreads information to all other nodes. Formula (B2) for $i=j$,

$$Q^\dagger_{jj} = \frac{1}{N}\sum_{i=1}^N \omega_{ij} - \frac{\widetilde{R}_G}{N^2} \tag{27}$$

indicates that $Q^\dagger_{jj}$ equals the average effective resistance from node j to all other nodes in G minus the overall graph's mean effective resistance [see (10)]. Furthermore, (27) illustrates that the electrically best connected node k^* minimizes the diagonal element in $Q^\dagger$, thus $Q^\dagger_{k^*k^*} \leqslant Q^\dagger_{jj}$ for any $1\leqslant j\leqslant N$. Another argument from the injection of a current I_c in node j, while all others are sinks, leads to a current vector $x = I_c(e_j - \frac{1}{N}u)$ with components $x_k = -\frac{I_c}{N}$ for $k\neq j$ and $x_j = \frac{(N-1)}{N}I_c$. The

[6] For a set of numbers $x_1, x_2, \ldots, x_n$, the arithmetic mean M_A is defined as $M_A = \frac{1}{n}\sum_{i=1}^n x_i$, while the geometric M_G is defined as $M_G = \sqrt[n]{\prod_{i=1}^n x_i}$ (see Ref. [16, p. 99]). This implies that $V_G^{\frac{2}{N-1}}$, a monotonically increasing function of V_G corresponds to the geometric mean. Both means satisfy the harmonic-geometric-arithmetic inequality (D2).

voltage/potential vector $v = Q^\dagger x$ in (6) then equals for a unit current $I_c = 1$ A

$$v = Q^\dagger\Big(e_j - \frac{u}{N}\Big) = Q^\dagger e_j = \mathrm{col}_j\, Q^\dagger$$

and

$$v_j = Q^\dagger_{jj} \tag{28}$$

is the largest positive potential in $\mathrm{col}_j\, Q^\dagger$, as follows physically. The proof that $Q^\dagger_{jj} \geqslant Q^\dagger_{kj}$ for any $1 \leqslant k \leqslant N$ is given in Corollary 1 in Sec. B. Since we have chosen as reference in Sec. II the average potential $v_{av} = \frac{1}{N}\sum_{i=1}^N v_i$ equal to zero, we can reinterpret (28) slightly more generally as

$$Q^\dagger_{jj} = v_j - v_{av} = \frac{1}{N}\sum_{i=1}^{N}(v_j - v_i),$$

indicating that the best spreader node minimizes the sum of the *potential differences* between its potential v_j and all other nodal potentials. This interpretation coincides with the "closeness" minimization of the average distance to all other nodes (see Sec. III B): The best connected node lies in the center of gravity.

In summary, node $k^* = \arg\min_{1\leqslant j\leqslant N}(Q^\dagger_{jj})$ can be regarded as the best diffuser of a flow to the rest of the network, in case a flow (of information or current) is injected in that node. To some extent, node k^* is most influential with respect to a diffusion operation in the network. In a Markov process, the node k^* in the Markov graph of all states can be regarded as the best, dynamically connected, state, through which the highest probability flux streams towards all other states. In a random walk (Sec. II), for example, the optimal spreader node k^* possesses the lowest average commute time to all other nodes, since $k^* = \arg\min_{1\leqslant j\leqslant N} e_j^T \Omega u = \arg\min_{1\leqslant j\leqslant N} e_j^T C u$.

The extension to the best spreader *pair* of nodes in a graph G is more complicated. Similarly as above, we now inject a current $\frac{I_c}{2}$ in node i and node j, while all other nodes are sinks, resulting in a current vector $x = I_c(\frac{1}{2}e_i + \frac{1}{2}e_j - \frac{1}{N}u)$ with components $x_k = -\frac{I_c}{N}$ for $k \notin \{i,j\}$ and $x_i = x_j = (\frac{1}{2} - \frac{1}{N})I_c$. From (6) and a unit current $I_c = 1$ A, the voltage vector is

$$\begin{aligned} v &= Q^\dagger\left(\frac{1}{2}e_i + \frac{1}{2}e_j - \frac{u}{N}\right) = \frac{1}{2}Q^\dagger e_i + \frac{1}{2}Q^\dagger e_j \\ &= \frac{1}{2}(\mathrm{col}_i\, Q^\dagger + \mathrm{col}_j\, Q^\dagger), \end{aligned}$$

from which the voltage $v_k = \frac{1}{2}(Q^\dagger_{ik} + Q^\dagger_{jk})$ of node $k \notin \{i,j\}$, while $v_i = \frac{1}{2}(Q^\dagger_{ii} + Q^\dagger_{ji}) \geqslant 0$ and $v_j = \frac{1}{2}(Q^\dagger_{ij} + Q^\dagger_{jj}) \geqslant 0$. The diagonal elements $Q^\dagger_{ii}$ of the pseudoinverse Laplacian $Q^\dagger$ are always non-negative [see (B1)], in fact, positive in a connected graph by (B9), and the largest in their row or column (Corollary 1), while the off-diagonal elements $Q^\dagger_{ij} = Q^\dagger_{ji}$ can be positive as well as negative (see the discussion after Theorem 6 in Appendix B). Hence, the potential-voltage sum $v_i + v_j$ is positive, reflecting a joint emission from each node in the pair (i,j), while all other nodes in the graph are receiving the diffusive items or information. Given the current injection vector $x = \frac{1}{2}e_i + \frac{1}{2}e_j - \frac{1}{N}u$ [that obeys the conservation law (4)], the best spreader pair (i,j) in the graph minimizes the non-negative potential/voltage sum $v_i + v_j$, which is equivalent to $\min_{\{i,j\}\in\mathcal{N}}(\frac{Q^\dagger_{ii}+Q^\dagger_{jj}}{2} + Q^\dagger_{ij})$. Since $Q^\dagger_{ij}$ can posses either sign, the introduction of (B8) results in the objective function to be minimized,

$$\min_{\{i,j\}\in\mathcal{N}}(v_i + v_j) = \min_{\{i,j\}\in\mathcal{N}}\big(Q^\dagger_{ii} + Q^\dagger_{jj} - \tfrac{1}{2}\omega_{ij}\big),$$

from which a lower bound follows as

$$\min_{\{i,j\}\in\mathcal{N}}(v_i + v_j) \geqslant \min_{\{i,j\}\in\mathcal{N}}(Q^\dagger_{ii} + Q^\dagger_{jj}) - \tfrac{1}{2}\max_{\{k,l\}\in\mathcal{N}}(\omega_{kl}).$$

If equality in the lower bound can be attained for the node pair (i,j) equal to the pair (k,l), then the lower bound shows that the best *possible* spreader pair (i,j) minimizes the sum $Q^\dagger_{ii} + Q^\dagger_{jj}$ of two elements in the ζ vector in (8) and, at the same time, has the largest effective resistance ω_{ij} between themselves. The latter means that the best spreader pair, in which each node is *individually* optimally "connected" to all other nodes, is *mutually* badly interconnected or well separated in the graph.[7] While the determination of the kth best spreader only consisted in a ranking of the elements in the ζ vector in (8), finding the best spreader *pair* is clearly more involved and hints to NP-completeness (see Sec. V): Just determining the best and second best spreader $[\min_{\{i,j\}\in\mathcal{N}}(Q^\dagger_{ii} + Q^\dagger_{jj})]$ by ranking the ζ vector is insufficient; also their mutual connectedness (ω_{ij}) in the graph matters. A further extension to find the best triplet of nodes or best set of m nodes exhibits the same requirement of satisfying a combined minimizing and maximizing part of the objective function, which is a disguise of the NP-completeness of the optimization problem.

V. THE ζ VECTOR AS A GRAPH METRIC VECTOR

Characterizing a network by a small set of metrics that are relatively easy to compute and to understand lies at the heart of network science. Many reviews [30–32] and books [16,33–38] cover graph metrics, real numbers that can be computed from the knowledge of the graph only (e.g., via its adjacency matrix). Each graph metric represents and quantifies a certain property of the graph. Here we propose the ζ vector in (8) as a promising graph metric vector that quantifies the nodal spreading capacity and we compare the ζ vector with other graph vectors in Sec. V B. The nature of a graph metric restricts us to demonstrate superiority of one established metric over another in all graphs, which complicates the reduction of the zoo of metrics to a basic set from which all others can be derived. Each graph metric views the graph through its own lenses and tells its limited story about the graph, much like Plato's famous "Allegory of the Cave."

Conceptually, the diagonal element $Q^\dagger_{jj}$ is most related to the closeness c_j. The closeness c_j measures the total number of hops in the shortest path tree rooted at a node j and is precisely equal to $c_j = (\Omega u)_j = N Q^\dagger_{jj} + \frac{R_G}{N}$ in an unweighted tree, where there is only one path from each node to each other

[7] The best spreader pair optimization problem, consisting of both a minimizing and maximizing part, makes intuitively sense when thinking, for instance, about the best heat diffusion in a room with two fireplaces.

node. In a graph with cycles, the closeness $c_j \geqslant Q^\dagger_{jj}$, because the closeness constraints traffic to follow only a shortest path, whereas $Q^\dagger_{jj}$ allows traffic to flow over all possible paths. In the terminology of optimization theory and linear programming, the vector ζ is called a *relaxation* of the closeness vector c, since the one-path constraint is removed in ζ. Moreover, as demonstrated here, the vector ζ is founded on solid matrix theory and is more analytically manageable than the closeness vector c, even if the network is perturbed (i.e., by adding or removing a link) as shown in Ref. [10].

Kitsak *et al.* [39] have proposed the coreness (also called k-core or k-shell) as the best metric to find the most influential spreader in a graph. Morone and Makse [40] proposed a percolation type of solution to the problem of finding the smallest set of nodes, whose removal fragments the network. Although that problem is NP-complete, accurate greedy methods exist as demonstrated by Kempe *et al.* [41] based on submodular functions.[8] Morone and Makse [40] introduced the collective influence, a graph metric related to the expansion around a node j up to h hops multiplied by the degree $d_j - 1$. They reported that their heuristic based on collective influence outweighs the strategies based on sequentially removing nodes with the highest degree, k-core, principal eigenvector component, closeness and page rank.

Figure 1 illustrates that the betweenness, closeness, and ζ vector perform similarly in a strategy to disconnect a graph and question whether a single metric can outperform others in an NP-complete problem. Strategies that determine the set of m links, whose removal minimizes the spectral radius of the adjacency matrix or, equivalently, maximizes the lower bound on the epidemic threshold, are evaluated in Ref. [42], while the influence of altering the assortativity on the spectral radius and algebraic connectivity of a graph are investigated in Ref. [43]. The correlation between the centrality metrics such as betweenness, principal eigenvector, closeness, leverage, k-shell index (a variant of k-core), and the degree mass is studied in Ref. [44] and a graph of metric correlations is proposed in Ref. [45]. The betweenness distribution in weighted networks as here is analyzed in Ref. [46], while Hernandez *et al.* [47] relates several variants of the weighted betweenness to the algebraic connectivity μ_{N-1}.

A. Variance of the ζ vector and bounds on the effective graph resistance R_G

Alternative forms and bounds for the diagonal elements $Q^\dagger_{jj}$ of the weighted pseudoinverse matrix $Q^\dagger$ are derived in Appendix B. Summing the expression (B1) for $Q^\dagger_{jj}$ over all nodes j and invoking the orthogonality condition $\sum_{j=1}^N (\widetilde{z}_k)_j^2 = 1$

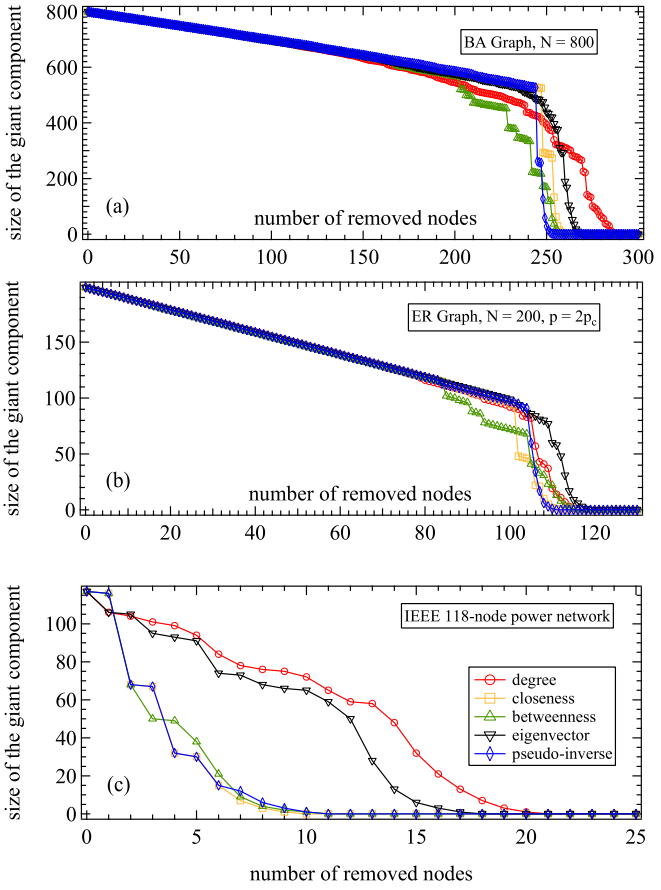

FIG. 1. The size of the giant component in three graphs: (a) a Barbasi-Albert graph with $N = 800$, (b) an Erdos-Renyi graph with $N = 200$ nodes, and (c) the IEEE 118 power grid both with $N = 118$ versus the removal of nodes according to five different strategies: The node with optimal graph metric, computed in each resulting graph, is removed.

for each integer subscript $1 \leqslant k \leqslant N$ referring to the kth eigenmode of $\widetilde{Q}$ with eigenvalue $\widetilde{\mu}_k$ yields

$$\sum_{j=1}^N Q^\dagger_{jj} = \sum_{k=1}^{N-1} \widetilde{\mu}_k^{-1} \sum_{j=1}^N (\widetilde{z}_k)_j^2 = \sum_{k=1}^{N-1} \widetilde{\mu}_k^{-1} = \frac{\widetilde{R}_G}{N},$$

where in the last step the definition (13) of the effective graph resistance $\widetilde{R}_G$ is used. Thus, the scaled effective graph resistance $\frac{\widetilde{R}_G}{N^2}$ can be regarded as the average over all nodes of the spreading capacity of an individual node. Clearly, the best and worst electrical spreader obey

$$\min_{1\leqslant j\leqslant N} (Q^\dagger_{jj}) \leqslant \frac{\widetilde{R}_G}{N^2} \leqslant \max_{1\leqslant j\leqslant N} (Q^\dagger_{jj}).$$

This interpretation suggests that we consider the variance of the vector $\zeta = (Q^\dagger_{11}, \ldots, Q^\dagger_{NN})$,

$$\mathrm{Var}[\zeta] = \frac{1}{N}\sum_{j=1}^N \left(Q^\dagger_{jj} - \frac{\widetilde{R}_G}{N^2}\right)^2 = \frac{1}{N}\sum_{j=1}^N (Q^\dagger_{jj})^2 - \frac{\widetilde{R}_G^2}{N^4},$$

[8] A submodular function f satisfies $f(S \cup \{v\}) - f(S) \geqslant f(T \cup \{v\}) - f(T)$ for all elements v and all pairs of sets $S \subseteq T$, which formally describes a "diminishing returns" property: The marginal gain from adding an element v to a set S is at least as high as the marginal gain from adding the same element to a superset T of S. The distance matrix H and effective resistance matrix Ω are submodular matrices (each element is a submodular function), where S is a subgraph of the graph T.

that measures the deviation of the individual, nodal spreading capacity from the mean $\frac{\widetilde{R}_G}{N^2}$ in the graph. Since

$$(Q^{\dagger 2})_{jj} = \sum_{k=1}^{N} Q^{\dagger}_{jk} Q^{\dagger}_{kj} = \sum_{k=1}^{N} (Q^{\dagger}_{jk})^2 = (Q^{\dagger}_{jj})^2 + \sum_{k=1;k\neq j}^{N} (Q^{\dagger}_{jk})^2,$$

the Cauchy-Schwarz inequality [16, p. 109], combined with $Q^{\dagger}u = 0$,

$$Q^{\dagger}_{jj} = -\sum_{k=1;k\neq j}^{N} Q^{\dagger}_{jk} \leqslant \sqrt{(N-1)\sum_{k=1;k\neq j}^{N} (Q^{\dagger}_{jk})^2},$$

leads to the inequality $(Q^{\dagger 2})_{jj} \geqslant (1+\frac{1}{N-1})(Q^{\dagger}_{jj})^2$. After summing over all j or taking the trace,[9]

$$\frac{N-1}{N}\sum_{k=1}^{N-1} \widetilde{\mu}_k^{-2} = \frac{N-1}{N}\sum_{j=1}^{N} (Q^{\dagger 2})_{jj} \geqslant \sum_{j=1}^{N} (Q^{\dagger}_{jj})^2,$$

we arrive at

$$\mathrm{Var}[\zeta] \leqslant \frac{\blacktriangledown_R}{N^2},$$

where

$$\blacktriangledown_R = (N-1)\sum_{k=1}^{N-1} \frac{1}{\widetilde{\mu}_k^2} - \left(\sum_{k=1}^{N-1} \frac{1}{\widetilde{\mu}_k}\right)^2. \tag{29}$$

In summary, the maximum possible variance $\frac{\blacktriangledown_R}{N^2}$ or the maximum standard deviation $\frac{\sqrt{\blacktriangledown_R}}{N}$ in the nodal spreading capacity from the overall average, equal to the scaled effective graph resistance $\frac{\widetilde{R}_G}{N^2}$, can be regarded as a companion graph metric to $\widetilde{R}_G$ that further specifies $\widetilde{R}_G$. In particular, $\blacktriangledown_R$ quantifies the graph's heterogeneity in spreading capacity and reflect how good the effective graph resistance $\widetilde{R}_G$ alone is representable because, as $\sqrt{\mathrm{Var}[\zeta]} \leqslant \max_{1\leqslant j\leqslant N}(Q^{\dagger}_{jj}) - \min_{1\leqslant j\leqslant N}(Q^{\dagger}_{jj})$, most of the nodes have a spreading capacity lying the interval $(\frac{\widetilde{R}_G}{N^2} - \sqrt{\mathrm{Var}[\zeta]}, \frac{\widetilde{R}_G}{N^2} + \sqrt{\mathrm{Var}[\zeta]}) \subset (\frac{\widetilde{R}_G - N\sqrt{\blacktriangledown_R}}{N^2}, \frac{\widetilde{R}_G + N\sqrt{\blacktriangledown_R}}{N^2})$. If $\blacktriangledown_R$ is large, then there is a large difference between the best and worst spreader node in the graph, while a small $\blacktriangledown_R$ points to a homogeneous network, in which nearly all nodes spread traffic (or information) equally well. For example, in the complete graph K_N, where $\mu_k = N$ for $1 \leqslant k < N$, we find that $\blacktriangledown_R = 0$. Finally, if the bound $\blacktriangledown_R$ in (29) of the variance $\mathrm{Var}[\zeta]$ is sharp and if ζ is approximately normal distributed, then we may roughly estimate the best spreader capacity [e.g. its lowest voltage as in (28)] by

$$\min_{1\leqslant j\leqslant N}(Q^{\dagger}_{jj}) \approx \frac{\widetilde{R}_G}{N^2} - \frac{\sqrt{\blacktriangledown_R}}{N}.$$

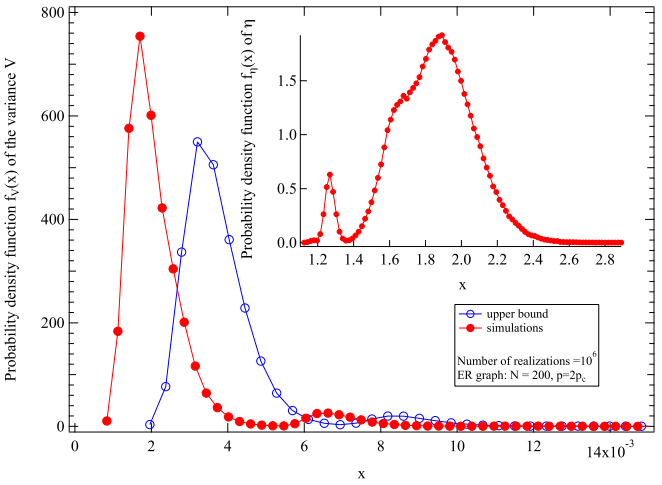

FIG. 2. The probability density function $f_V(x)$ of the variance $V = \mathrm{Var}[\zeta]$ and its the upper bound $\frac{\blacktriangledown_R}{N^2}$ in the unweighted Erdős-Rényi (ER) random graph $G_p(N)$ with $N = 200$ nodes and link density $p = 2p_c$ for 10^6 realizations. The insert shows the corresponding pdf of the ratio $\eta = \frac{\blacktriangledown_R}{N^2\mathrm{Var}[\zeta]}$.

Figure 2 compares the variance $\mathrm{Var}[\zeta]$ and the upper bound $\frac{\blacktriangledown_R}{N^2}$, as well as their ratio η, in the unweighted Erdős-Rényi (ER) random graph $G_p(N)$ with $N = 200$ nodes and link density $p = 2p_c$ (where the critical link density $p_c \sim \frac{\ln N}{N}$ for large N) for 10^6 realizations, illustrating that the upper bound is reasonably close, and, on average, less than a factor of 2 off.

More surprising in Fig. 3 is the good approximation $\frac{R_G}{N^2} - \frac{\sqrt{\blacktriangledown_R}}{N}$ for $m = \min_{1\leqslant j\leqslant N}(Q^{\dagger}_{jj})$ as well as the forbidden

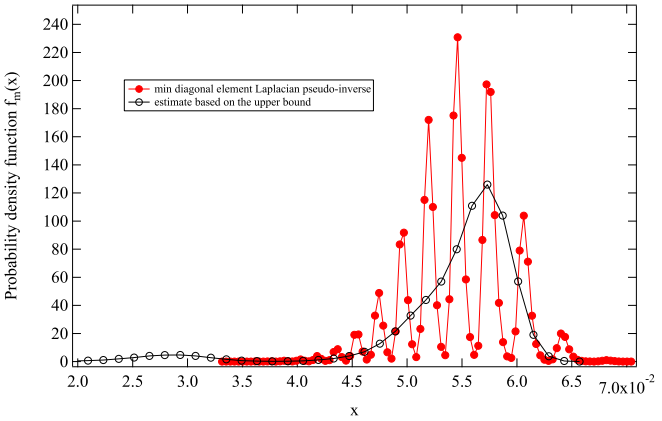

FIG. 3. The probability density function of $m = \min_{1\leqslant j\leqslant N} Q^{\dagger}_{jj}$ and its estimate $\frac{R_G}{N^2} - \frac{\sqrt{\blacktriangledown R}}{N}$ for the same realizations as in Fig. 2.

[9] Using (B1), we have that

$$\sum_{j=1}^{N}(Q^{\dagger}_{jj})^2 = \sum_{k=1}^{N-1}\sum_{l=1}^{N-1}\widetilde{\mu}_l^{-1}\widetilde{\mu}_k^{-1}\sum_{j=1}^{N}((\widetilde{z}_k)_j(\widetilde{z}_l)_j)^2.$$

Invoking the Cauchy-Schwarz inequality and the orthogonality of eigenvectors

$$\sum_{j=1}^{N}((\widetilde{z}_k)_j(\widetilde{z}_l)_j)^2 \geqslant \frac{1}{N}\left(\sum_{j=1}^{N}(\widetilde{z}_k)_j(\widetilde{z}_l)_j\right)^2 = \frac{1}{N}\delta_{kl}$$

yields $\sum_{j=1}^{N}(Q^{\dagger}_{jj})^2 \geqslant \frac{1}{N}\sum_{k=1}^{N-1}\widetilde{\mu}_k^{-2}$, while (B9) leads to $\sum_{j=1}^{N}(\widehat{Q}^{-1}_{jj})^2 \geqslant (1-\frac{1}{N})^4\sum_{j=1}^{N}\frac{1}{d_j^2}$.

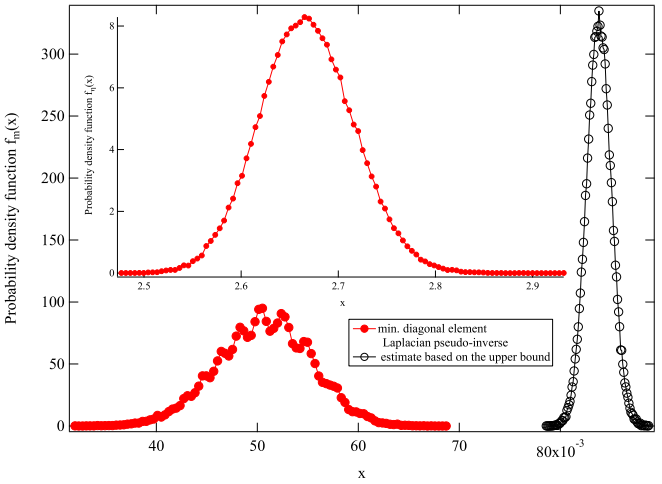

FIG. 4. The probability density function of $m = \min_{1\leqslant j\leqslant N} Q^{\dagger}_{jj}$ and its estimate $\frac{R_G}{N^2} - \frac{\sqrt{\blacktriangledown_R}}{N}$ for 10^5 realizations of a Barabasi-Albert graph on $N = 500$ nodes as described in Fig. 6. The insert shows the corresponding pdf of the ratio $\eta = \frac{\blacktriangledown_R}{N^2 Var[\zeta]}$.

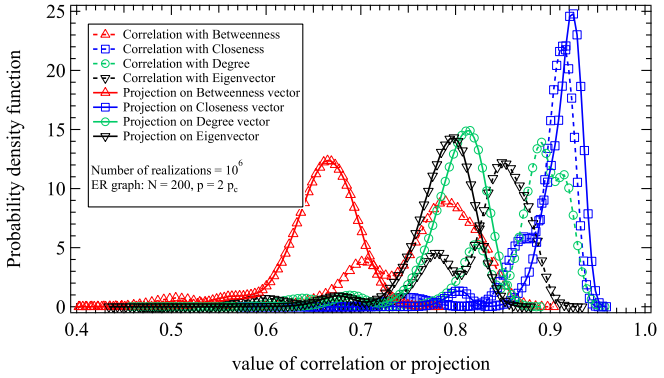

FIG. 5. The probability density function $f_Y(x)$ of the random variable Y, which is either a projection or a correlation, in the unweighted ER random graph $G_p(N)$ with $N = 200$ nodes and link density $p = 2p_c$. Since all considered linear correlation coefficients are negative, their absolute value has been plotted in order to better compare with the projections.

values of $m = \min_{1\leqslant j\leqslant N} (Q^{\dagger}_{jj})$ in the unweighted ER random graph $G_{2p_c}(200)$, reflected by the oscillations in the probability density function $f_m(x)$ versus the values x. For certain x values, $f_m(x)$ tends to zero, which means that these values cannot occur almost surely.

At the moment, we do not have a precise explanation why certain values of $m = \min_{1\leqslant j\leqslant N} (Q^{\dagger}_{jj})$ in the unweighted ER random graph $G_{2p_c}(200)$ are forbidden almost surely. Oscillations also occur in the other components of ζ, as well as in ER graphs with precisely L links and N nodes. Since the diagonal elements (B1) of the Laplacian pseudoinverse depend on the eigenvector components (as well as the eigenvalues), Fig. 3 suggests the occurrence of possible restrictions on the eigenvectors in $G_{2p_c}(200)$, because the eigenvalues [appearing the upper bound in (29)] do not seem to be confined (black line in Fig. 3).

Figure 4 plots $m = \min_{1\leqslant j\leqslant N} (Q^{\dagger}_{jj})$ in the unweighted Barabási-Albert (BA) random graphs on $N = 500$ nodes and illustrates that our approximation $\frac{R_G}{N^2} - \frac{\sqrt{\blacktriangledown_R}}{N}$ for $m = \min_{1\leqslant j\leqslant N} (Q^{\dagger}_{jj})$ is less accurate than in ER random graphs, although the ratio $\eta = \frac{\blacktriangledown_R}{N^2 \mathrm{Var}[\zeta]}$ (in the insert) is similar to that in ER random graphs (insert in Fig. 2). Moreover, clear forbidden values are less pronounced as the amplitude of oscillations in the probability density function $f_m(x)$ are much smaller. Thus, while power-law characteristics usually lead to the more exotic behavior, here, the regularity and homogeneity of ER random graphs produce fascinations.

The theory in Appendix B suggests to relate $m = \min_{1\leqslant j\leqslant N} (Q^{\dagger}_{jj})$ to the inverse of the maximum degree $\frac{1}{d_{\max}}$. The peaks in Fig. 3 in ER graph $G_{2p_c}(200)$ indeed correspond to inverses $\frac{1}{d_i}$ of the degree and, in the majority of the realizations (about 70%), the node j that minimizes $Q^{\dagger}_{jj}$ also possesses the largest degree. In power-law graphs, this correspondence is less pronounced. A possible explanation is the fairly localized value of the maximum degree in ER random graphs, in contrast to the broader distribution of $d_{\max}$ in power-law random graphs.

B. Evaluation of the vector $\zeta = (Q^{\dagger}_{11}, \ldots, Q^{\dagger}_{NN})$

Several nodal "centrality" metrics are compared with the vector $\zeta = (Q^{\dagger}_{11}, \ldots, Q^{\dagger}_{NN})$, whose jth component $Q^{\dagger}_{jj}$ measures how good node j spreads information to all other nodes. Figure 5 shows the probability density function $f_Y(x)$ of either a correlation or projection between a known centrality vector and the nodal spreader vector ζ. For example, the linear correlation coefficient $Y = \rho(\zeta, d) = \frac{E[\zeta d] - E[d]E[\zeta]}{\sqrt{\mathrm{Var}[\zeta]\mathrm{Var}[d]}}$ between the degree vector d and the vector ζ is compared to the projection $d^T\zeta$ for 10^6 realizations of the unweighted ER random graph $G_p(N)$ with $N = 200$ nodes and link density $p = 2p_c$. Next to the principal eigenvector x_1 of the adjacency matrix A belonging to the largest eigenvalue $\lambda_1(A)$ and the degree vector $d = Au$, we considered also the nodal betweenness vector b, defined in Ref. [47] and the closeness vector c, defined in Ref. [16, Eq. (15.7) on p. 370]. All considered centrality vectors have non-negative components so that the mutual projections or scalar products are positive. The betweenness b_i of a node i is defined as the total number of shortest paths between all possible pairs of nodes in the graph that traverse the node i,

$$b_i = \sum_{k=1}^{N} \sum_{m=1}^{N} 1_{\{i\in\mathcal{P}^*_{km}\}},$$

where the indicator function $1_{\{X\}} = 1$ if X is true, otherwise $1_{\{X\}} = 0$, and where $\mathcal{P}^*_{km}$ is the shortest path (denoted by *) between node k and m.

Figure 5 shows that the closeness vector c is "closest" to the vector ζ, because both $E[\rho(\zeta, c)]$ and $E[c^T\zeta]$ exceed the others (the peaks of the blue curve corresponds to the highest x values). Except for the closeness, Fig. 5 illustrates that the average correlation is larger than the average projection. Figure 5 also shows that most pdfs are not unimodal. The precise reason for the appearance of several local maxima is unclear, but it points to the fact that the vector ζ is not easily

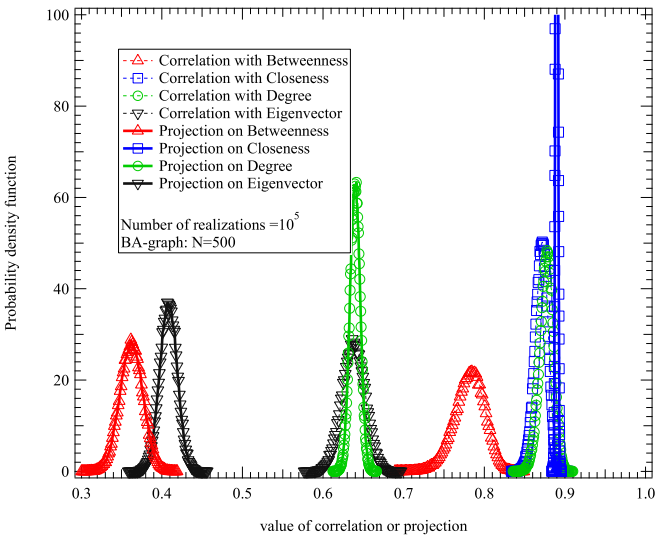

FIG. 6. The probability density function $f_Y(x)$ of the random variable Y, which is either a projection or a correlation, in the unweighted Barabasi-Albert graph with $N = 500$ nodes, generated from a set of 5 initially completely connected nodes and each new node connects to 3 previous nodes in the graph. Since all considered linear correlation coefficients are negative, their absolute value has been plotted in order to better compare with the projections.

interchanged by another nodal centrality vector, which may justify a study of the vector ζ, as presented here. The situation in the Barabási-Albert graph in Fig. 6 closely follows that in the ER random graph $G_{2p_c}(200)$ in Fig. 5: Correlations are higher than projections, except for the closeness, but the range on the x axis is broader, though narrower and unimodal around the peaks, that are higher compared to ER graphs.

VI. CONCLUSION

Inspired by electrical current flows that satisfy conservation laws, the weighted Laplacian $\widetilde{Q}$ and its pseudoinverse $Q^\dagger$ are argued to be fundamental vehicles to explore properties of graphs as well as dynamic processes in networks. New matrix relations are presented as well as connections between the effective resistance matrix Ω as a distance matrix and its corresponding volume that reflects the number of weighted spanning trees. The best electrical spreader, defined as the node whose component in the vector ζ in (8), containing the diagonal elements of the pseudoinverse $Q^\dagger$, is minimum, has the lowest energy or potential in the network and is thus best connected to all other nodes. The vector ζ can thus be considered as a graph vector that was compared to other centrality vectors such as the degree d, closeness c, betweenness b, and principal eigenvector x of the adjacency matrix. As expected, the correlation and projection of vector ζ and the closeness vector c are the highest. Remarkable oscillations in the potential value of the best spreader, stronger in an ER graph than in a BA graph, were observed in Fig. 3 that point to forbidden regions. Sequentially removing the best spreader nodes in the resulting graph (or removing nodes according to the rank in the vector ζ) is expected to be a good strategy to fragment the graph. Conversely, protecting the best spreader nodes in a network will result in a robustly designed network.

ACKNOWLEDGMENT

We are very grateful to Xiangrong Wang and Zhidong He for their comments on an earlier version.

APPENDIX A: PROOFS OF THEOREMS 1 TO 3

Proof of Theorem 1. Consider the effect of an external current vector $x = I_c(e_m - e_n)$, injected in node m and leaving the circuit at node n, on the voltage difference $v_{ab} = v_a - v_b$ between node a and b. The inverse relation (6) indicates that

$$v_{ab} = I_c(e_a - e_b)^T Q^\dagger (e_m - e_n),$$

while the definition (9) of the effective resistance $\omega_{ab} = \frac{v_{ab}}{I_c}|_{m=a;n=b} = (e_a - e_b)^T Q^\dagger (e_a - e_b)$. The definition (7) of the effective graph resistance shows that

$$(e_a - e_b)^T \Omega (e_m - e_n) = -2(e_a - e_b)^T Q^\dagger (e_m - e_n)$$

so that

$$v_{ab} = -\tfrac{1}{2} I_c (e_a - e_b)^T \Omega (e_m - e_n) \tag{A1}$$

for any pair with injecting node m and leaving node $n \neq m$. Choosing the pair $m = a$ and $n = b$, we thus find an alternative expression of the effective resistance $\omega_{ab} = e_a^T \Omega e_b$ as

$$\omega_{ab} = -\tfrac{1}{2}(e_a - e_b)^T \Omega (e_a - e_b), \tag{A2}$$

mainly due to the fact that $\omega_{jj} = 0$.

We can consider a more general external current vector x. The conservation law (4) of external current, $u^T x = 0$, illustrates that the vector x can always be written as a linear combination of $(e_m - e_n)$ couples. Since Eq. (A1) is linear in the vector $(e_m - e_n)$, the resulting potential difference v_{ab} from such a general external current vector x is given by

$$v_{ab} = -\tfrac{1}{2}(e_a - e_b)^T \Omega x,$$

which treats voltage differences only. Rewritten for an individual voltage yields $v_a = -\frac{1}{2} e_a^T \Omega x + c$, where c is a constant that does not depend on the node a and which becomes in vector form $v = -\frac{1}{2}\Omega x + cu$. Since we have assumed that the average voltage $v_{\rm av} = 0$ or $u^T v = 0$, we obtain $u^T v = -\frac{1}{2} u^T \Omega x + c u^T u = 0$ from which $c = \frac{1}{2N} u^T \Omega x$. Introduced into $v = -\frac{1}{2}\Omega x + uc$ and invoking $J = uu^T$ yields

$$v = -\frac{1}{2}\Omega x + \frac{1}{2N} uu^T \Omega x = \frac{1}{2}\left(\frac{1}{N} J - I\right)\Omega x.$$

Finally, since $Q_{K_N} = NI - J$, we arrive at (14). ■

Proof of Theorem 2. From (6), we have $v = Q^\dagger x = (\widetilde{Q} + \alpha J)^{-1} x$. Additionally, (14) states $v = -\frac{1}{2N} Q_{K_N} \Omega x$ for $u^T x = 0$. Combining both equations and $Q_{K_N} = NI - J$ gives

$$\begin{aligned} x &= \frac{1}{2N}(\widetilde{Q} + \alpha J)(J - NI)\Omega x \\ &= \frac{1}{2N}(\widetilde{Q} J + \alpha J^2 - \alpha N J I - N \widetilde{Q})\Omega x. \end{aligned}$$

Using $\widetilde{Q} J = (\widetilde{Q} u) u^T = 0$ and $J^2 = NJ$, leads to (15). ■

Proof of Theorem 3. For a general vector a and scalar s in the right-hand side of (21), we expand the block determinant along the first row in cofactors, followed by a cofactor expansion of the remaining first column,

$$\det\left[\begin{array}{c|c} s & a^T \\ \hline a & \widetilde{Q} \end{array}\right] = s\det\widetilde{Q} + \sum_{i=1}^{N}(-1)^{i+1}a_i \times \sum_{j=1}^{N}(-1)^j a_j \det(\widetilde{Q}_{\setminus \text{row}\, i \setminus \text{col}\, j}).$$

Since the number of weighted spanning trees $\widetilde{\xi} = (\text{adj}\widetilde{Q})_{ij} = (-1)^{i+j}\det(\widetilde{Q}_{\setminus \text{row}\, i \setminus \text{col}\, j})$ for each element [2, art. 82] and $\det(\widetilde{Q}) = 0$, the above simplifies to

$$\det\left[\begin{array}{c|c} s & a^T \\ \hline a & \widetilde{Q} \end{array}\right] = -\widetilde{\xi}\sum_{i=1}^{N}\sum_{j=1}^{N}a_i a_j = -\widetilde{\xi}(u^T a)^2.$$

Let $s = \zeta^T Q\zeta + \frac{4R_G}{N^2}$ and $a = -(\widetilde{Q}\zeta + \frac{2}{N}u)$ be the eigenvector of $\widetilde{Q}\Omega$ belonging to the zero eigenvalue, so that we find

$$\det\left[\begin{array}{c|c} \zeta^T Q\zeta + \frac{4R_G}{N^2} & -(\widetilde{Q}\zeta + \frac{2}{N}u)^T \\ \hline -(\widetilde{Q}\zeta + \frac{2}{N}u) & \widetilde{Q} \end{array}\right] = -4\widetilde{\xi}.$$

Using the inverse block matrix relation (21) and determinant rules, the Cayley-Menger determinant of Ω is

$$\det\left[\begin{array}{c|c} 0 & u^T \\ \hline u & \Omega \end{array}\right] = \frac{(-1)^N 2^{N-1}}{\widetilde{\xi}},$$

which leads to (24), after using the simplex' volume (22). ■

APPENDIX B: DIAGONAL ELEMENTS OF THE PSEUDOINVERSE $Q^\dagger$ OF THE WEIGHED LAPLACIAN $\widetilde{Q}$

We present different expressions and bounds for the diagonal element $Q^\dagger_{jj}$.

Theorem 4. Let $Q^\dagger$ denote the pseudoinverse matrix of the weighted Laplacian $\widetilde{Q}$ of a graph G. The expression

$$Q^\dagger_{jj} = \sum_{k=1}^{N-1}\widetilde{\mu}_k^{-1}(\widetilde{z}_k)_j^2 \tag{B1}$$

demonstrates that $Q^\dagger_{jj} \geqslant 0$. Any element of Laplacian pseudoinverse

$$Q^\dagger_{ij} = \frac{1}{2}\left(\frac{1}{N}\sum_{k=1}^{N}\omega_{ik} + \frac{1}{N}\sum_{k=1}^{N}\omega_{jk}\right) - \frac{1}{2}\omega_{ij} - \frac{\widetilde{R}_G}{N^2} \tag{B2}$$

equals $Q^\dagger_{ij} = -\frac{1}{2N}e_i^T Q_{K_N}\Omega(e_j - \frac{u}{N})$, which can be "electrically" measured by injecting a current into node j while all other nodes are sink and subsequently measuring the voltage at node i. For any number $\alpha \neq 0$, the jth diagonal element of $Q^\dagger$ corresponding to node j equals

$$Q^\dagger_{jj} = (\widetilde{Q} + \alpha J)^{-1}_{jj} - \frac{1}{\alpha N^2} = \frac{\det[\widetilde{Q}_{\setminus \text{row}\, j \setminus \text{col}\, j} + \alpha J_{(N-1)\times(N-1)}]}{\det(\widetilde{Q} + \alpha J_{N\times N})} - \frac{1}{\alpha N^2}, \tag{B3}$$

where $\widetilde{Q}_{\setminus \text{row}\, j \setminus \text{col}\, j}$ is the weighted Laplacian in which row j and col j are deleted. Another form is

$$Q^\dagger_{jj} = \frac{u^T(\widetilde{Q}_{\setminus \text{row}\, j \setminus \text{col}\, j})^{-1}u}{N^2}, \tag{B4}$$

where the quadratic form $u^T(\widetilde{Q}_{\setminus \text{row}\, j \setminus \text{col}\, j})^{-1}u$ equals the sum over all elements in $(\widetilde{Q}_{\setminus \text{row}\, j \setminus \text{col}\, j})^{-1}$.

Proof. First, (B1) follows directly from (11).

Second, we start from the definition of an element in a matrix M, $m_{ij} = e_i^T M e_j$, and invoke the property that $Q^\dagger u = 0$,

$$Q^\dagger_{ij} = e_i^T Q^\dagger e_j = \left(e_i - \frac{u}{N}\right)^T Q^\dagger\left(e_j - \frac{u}{N}\right).$$

Using $x^T Q^\dagger x = -\frac{1}{2}x^T\Omega x$ in (18), which holds for any vector x obeying $x^T u = 0$, we obtain

$$Q^\dagger_{ij} = -\frac{1}{2}\left(e_i - \frac{u}{N}\right)^T\Omega\left(e_j - \frac{u}{N}\right) = \frac{u^T\Omega}{2N}(e_i + e_j) - \frac{1}{2}\omega_{ij} - \frac{u^T\Omega u}{2N^2}.$$

With the definition (10) of the effective graph resistance $\widetilde{R}_G = \frac{u^T\Omega u}{2}$, we arrive at (B2).

Next, let us consider $Q^\dagger_{jj}$ in (12),

$$Q^\dagger_{jj} = \sum_{k=1}^{N}(\widetilde{Q} + \alpha J)^{-1}_{jk}\left(I - \frac{1}{N}J\right)_{kj} = -\frac{1}{N}\sum_{k=1}^{N}(\widetilde{Q} + \alpha J)^{-1}_{jk} + (\widetilde{Q} + \alpha J)^{-1}_{jj} = -\frac{1}{N}((\widetilde{Q} + \alpha J)^{-1}u)_j + (\widetilde{Q} + \alpha J)^{-1}_{jj}.$$

Since

$$\widetilde{Q} + \alpha J = \sum_{k=1}^{N-1}\widetilde{\mu}_k\widetilde{z}_k\widetilde{z}_k^T + \alpha N\widetilde{z}_N\widetilde{z}_N^T$$

with the normalized eigenvector $\widetilde{z}_N = \frac{u}{\sqrt{N}}$ (obeying $\widetilde{z}_N^T\widetilde{z}_N = 1$) belonging to eigenvalue $\widetilde{\mu}_N = \alpha N$, we have that $(\widetilde{Q} + \alpha J)^{-1} = \sum_{k=1}^{N-1}\widetilde{\mu}_k^{-1}\widetilde{z}_k\widetilde{z}_k^T + \frac{1}{\alpha N}\widetilde{z}_N\widetilde{z}_N^T$ and $\det(\widetilde{Q} + \alpha J) = \alpha N\prod_{k=1}^{N-1}\widetilde{\mu}_k$. Hence, we observe that $(\widetilde{Q} + \alpha J)^{-1}u = \frac{1}{\alpha N}u$, so that

$$Q^\dagger_{jj} = (\widetilde{Q} + \alpha J)^{-1}_{jj} - \frac{1}{\alpha N^2}.$$

Invoking the definition of the inverse of a matrix $B = \frac{\text{adj}B}{\det B}$, where the adjugate (or adjoint) adj$B$ is the transpose of the matrix of cofactors of B, yields (B3).

At last, we proof the expression (B4). Invoking [1]

$$(\widetilde{z}_k)_j^2 = \frac{\det(\widetilde{Q}_{\setminus \text{row}\, j \setminus \text{col}\, j} - \widetilde{\mu}_k I)}{\sum_{n=1}^{N}\det(\widetilde{Q}_{\setminus \text{row}\, n \setminus \text{col}\, n} - \widetilde{\mu}_k I)} = \frac{\det(\widetilde{Q}_{\setminus \text{row}\, j \setminus \text{col}\, j} - \widetilde{\mu}_k I)}{-c'_{\widetilde{Q}}(\widetilde{\mu}_k)}. \tag{B5}$$

For $k = N$ for which $\widetilde{z}_N = \frac{u}{\sqrt{N}}$ with corresponding eigenvalue $\widetilde{\mu}_N = 0$, we find that

$$\det(\widetilde{Q}_{\setminus \text{row } j \setminus \text{col } j}) = -\frac{c'_{\widetilde{Q}}(0)}{N} = -\frac{1}{N} c_1(\widetilde{Q}_G) = \frac{1}{N}\prod_{k=1}^{N-1}\widetilde{\mu}_k = \widetilde{\xi}. \tag{B6}$$

Using the "rank one update" formula [2, p. 256]

$$\det\left(A_{n\times n} + C_{n\times 1} D^T_{1\times n}\right) = \det A \det\left(1 + D^T_{1\times n} A^{-1} C_{n\times 1}\right)$$

yields

$$\det\left(\widetilde{Q}_{\setminus \text{row } j \setminus \text{col } j} + \alpha u_{N-1}.u^T_{N-1}\right) = \det(\widetilde{Q}_{\setminus \text{row } j \setminus \text{col } j})[1 + \alpha u^T (\widetilde{Q}_{\setminus \text{row } j \setminus \text{col } j})^{-1} u] \tag{B7}$$

so that (B3) becomes

$$Q^\dagger_{jj} = \frac{\det(\widetilde{Q}_{\setminus \text{row } j \setminus \text{col } j})[1 + \alpha u^T (\widetilde{Q}_{\setminus \text{row } j \setminus \text{col } j})^{-1} u]}{\det(\widetilde{Q} + \alpha J_{N\times N})} - \frac{1}{\alpha N^2}$$
$$= \frac{1}{\alpha}\left[\frac{\det(\widetilde{Q}_{\setminus \text{row } j \setminus \text{col } j})}{N\prod_{k=1}^{N-1}\widetilde{\mu}_k} - \frac{1}{N^2}\right] + \frac{\det(\widetilde{Q}_{\setminus \text{row } j \setminus \text{col } j}) u^T (\widetilde{Q}_{\setminus \text{row } j \setminus \text{col } j})^{-1} u}{N\prod_{k=1}^{N-1}\widetilde{\mu}_k}.$$

Using (B6) leads to (B4), which can also be proved by differentiation both sides of (B3) with respect to α. ■

The expression (B3) has an interesting form.[10] For an unweighted graph (and Laplacian Q with corresponding pseudoinverse $\widetilde{Q}^{-1}$), the number of all possible spanning trees in the graph [2, p. 76], called the complexity $\xi(G)$, equals

$$\det(Q + J_{N\times N}) = N^2 \xi(G).$$

Corollary 1. In each row (or column) of the pseudoinverse $Q^\dagger$, the diagonal element is the largest: $Q^\dagger_{ii} \geqslant Q^\dagger_{ij}$ for each row $1 \leqslant i \leqslant N$.

Proof. Taking the difference $Q^\dagger_{ii} - Q^\dagger_{ij}$ in (B2) and using $\omega_{ii} = 0$ gives

$$Q^\dagger_{ii} - Q^\dagger_{ij} = \frac{1}{2}\omega_{ij} + \frac{u^T\Omega}{2N}(e_i - e_j) = \frac{1}{2N}\sum_{k=1}^{N}\{\omega_{ki} - \omega_{kj} + \omega_{ij}\}.$$

Since each element in the effective resistance matrix Ω satisfies [3] the triangle inequality $\omega_{ki} + \omega_{ij} \geqslant \omega_{kj}$, we find, for any j,

$$Q^\dagger_{ii} - Q^\dagger_{ij} \geqslant 0,$$

implying that $Q^\dagger_{ii} \geqslant Q^\dagger_{ij}$, which ends the proof. ■

Bounds of the Hölder type (see Ref. [16, Sec. 5.5, Eq. (5.24)]), generalizing the triangle inequality $\omega_{ki} + \omega_{ij} \geqslant \omega_{kj}$, are discussed in Ref. [48]. Definition (7) shows that

$$u^T\Omega = u^T\zeta u^T + N\zeta^T = \frac{\widetilde{R}_G}{N}u^T + N\zeta^T$$

so that (B2) becomes

$$Q^\dagger_{ij} = \frac{Q^\dagger_{ii} + Q^\dagger_{jj}}{2} - \frac{1}{2}\omega_{ij}. \tag{B8}$$

For each positive semidefinite matrix P, it holds [16, p. 241] that $P_{ij} \leqslant \frac{P_{ii}+P_{jj}}{2}$, illustrating that (B8) provides the precise relation between off-diagonal elements in terms of the mean of two diagonal elements and a "correction" ω_{ij} equal to half the effective resistance between node i and j.

Theorem 5. Let $Q^\dagger$ denote the pseudoinverse of the weighted Laplacian $\widetilde{Q}$, and then the diagonal element $Q^\dagger_{jj}$ is lower bounded by

$$Q^\dagger_{jj} \geqslant \frac{1}{\widetilde{Q}_{jj}}\left(1 - \frac{1}{N}\right)^2 \tag{B9}$$

and, for each positive real number α, it holds that

$$\frac{\widetilde{Q}_{jj} + \alpha Q^\dagger_{jj}}{2} \geqslant \sqrt{\alpha}\left(1 - \frac{1}{N}\right). \tag{B10}$$

Proof. We multiply (B1) and

$$\widetilde{Q}_{jj} = \sum_{k=1}^{N-1}\widetilde{\mu}_k(\widetilde{z}_k)^2_j$$

and obtain

$$\widetilde{Q}_{jj}Q^\dagger_{jj} = \sum_{k=1}^{N-1}\sum_{l=1}^{N-1}\frac{\widetilde{\mu}_k}{\widetilde{\mu}_l}((\widetilde{z}_k)_j(\widetilde{z}_l)_j)^2 = \sum_{k=1}^{N-1}\sum_{l=1}^{k-1}\frac{\widetilde{\mu}_k}{\widetilde{\mu}_l}((\widetilde{z}_k)_j(\widetilde{z}_l)_j)^2 + \sum_{k=1}^{N-1}\sum_{l=k}^{N-1}\frac{\widetilde{\mu}_k}{\widetilde{\mu}_l}((\widetilde{z}_k)_j(\widetilde{z}_l)_j)^2.$$

After reversing the summation in the last equation

$$\sum_{k=1}^{N-1}\sum_{l=k}^{N-1}\frac{\widetilde{\mu}_k}{\widetilde{\mu}_l}((\widetilde{z}_k)_j(\widetilde{z}_l)_j)^2 = \sum_{l=1}^{N-1}\sum_{k=1}^{l}\frac{\widetilde{\mu}_k}{\widetilde{\mu}_l}((\widetilde{z}_k)_j(\widetilde{z}_l)_j)^2$$

and then changing the index $k \to l$ and $l \to k$, we have

$$\widetilde{Q}_{jj}Q^\dagger_{jj} = \sum_{k=1}^{N-1}\sum_{l=1}^{k-1}\left(\frac{\widetilde{\mu}_k}{\widetilde{\mu}_l} + \frac{1}{\frac{\widetilde{\mu}_k}{\widetilde{\mu}_l}}\right)((\widetilde{z}_k)_j(\widetilde{z}_l)_j)^2 + \sum_{k=1}^{N-1}(\widetilde{z}_k)^4_j.$$

[10] Whereas for an adjacency matrix, the removal of row j and column j implies that $A_{\setminus \text{row } j \setminus \text{col } j} = A_{G\setminus\{j\}}$, where $G\setminus\{j\}$ is the graph in which node j is removed, this property does not hold for the Laplacian, i.e., $Q_{\setminus \text{row } j \setminus \text{col } j} \neq Q_{G\setminus\{j\}}$, because $Q_{\setminus \text{row } j \setminus \text{col } j}u = a_j$ with the vector a_j is equal to the jth column (or row) of A and $\text{diag}(Q_{\setminus \text{row } j \setminus \text{col } j})$ contains the degrees of the graph G without degree d_j, while $Q_{G\setminus\{j\}}u = 0$ and $\text{diag}(Q_{G\setminus\{j\}})$ contains all the degrees of the graph $G\setminus\{j\}$. The interlacing theorem [2, p. 246] states that all eigenvalues of $Q_{\setminus \text{row } j \setminus \text{col } j}$ lie in between the eigenvalues of Q,

$$\mu_{m+1}(Q) \leqslant \mu_m(Q_{\setminus \text{row } j \setminus \text{col } j}) \leqslant \mu_m(Q) \quad \text{for } 1 \leqslant m \leqslant N-1,$$

while an analysis of the cone of $G\setminus\{j\}$ leads to (see Ref. [2, art. 116])

$$\mu_m(G\setminus\{j\}) + 1 \geqslant \mu_{m+1}(G) \qquad \text{for } 2 \leqslant m \leqslant N-1.$$

Since the function $t+\frac{1}{t} \geqslant 2$ for $t \geqslant 0$, we find the inequality

$$\widetilde{Q}_{jj} Q^{\dagger}_{jj} \geqslant 2 \sum_{k=1}^{N-1} \sum_{l=1}^{k-1} ((\widetilde{z}_k)_j (\widetilde{z}_l)_j)^2 + \sum_{k=1}^{N-1} (\widetilde{z}_k)_j^4 = \sum_{k=1}^{N-1} \sum_{l=1}^{N-1} (\widetilde{z}_k)_j^2 (\widetilde{z}_l)_j^2 = \left(1-\frac{1}{N}\right)^2,$$

which establishes the lower bound (B9). We can apply the same idea to

$$\widetilde{Q}_{jj} + \alpha Q^{\dagger}_{jj} = \sum_{k=1}^{N-1} \left(\widetilde{\mu}_k + \frac{\alpha}{\widetilde{\mu}_k}\right) (\widetilde{z}_k)_j^2.$$

Only when α is real and positive, the minimum of the function $f(t) = t + \frac{\alpha}{t}$ occurs $t = \sqrt{\alpha}$ with $f(\sqrt{\alpha}) = 2\sqrt{\alpha}$. Hence, we find the lower bound (B10) which complements the geometric mean inequality (B9). ■

Since both $\widetilde{Q}_{jj}$ and $Q^{\dagger}_{jj}$ are non-negative, the arithmetic mean upper bounds the geometric mean so that

$$\frac{\widetilde{Q}_{jj} + Q^{\dagger}_{jj}}{2} \geqslant \sqrt{\widetilde{Q}_{jj} Q^{\dagger}_{jj}} \geqslant \left(1-\frac{1}{N}\right).$$

There exists a large class of matrix function f that obey $f(\widetilde{Q}) = \sum_{k=1}^{N-1} f(\widetilde{\mu}_k) \widetilde{z}_k \widetilde{z}_k^T$. For this class of functions, we observe that the proof is readily generalized to any positive function f of a positive semidefinite matrix, such that

$$(f(\widetilde{Q}))_{jj} (f(Q^{\dagger}))_{jj} \geqslant \left(1-\frac{1}{N}\right)^2.$$

The bound (B9) thus seems widely applicable and bears some similarity to the famous Heisenberg uncertainty relation in quantum mechanics (see, e.g., Refs. [49,50]). The difference is that inequality (B9) lower bounds the product of any diagonal element in a semidefinite matrix with its pseudoinverse, instead of the product of variances of noncommuting operators in Heisenberg's uncertainty inequality. For an unweighted Laplacian Q, the lower bound (B9) simplifies to

$$(\widehat{Q}^{-1})_{jj} \geqslant \frac{1}{d_j}\left(1-\frac{1}{N}\right)^2, \tag{B11}$$

from which a lower bound for the effective graph resistance follows with (13) as

$$R_G \geqslant \frac{(N-1)^2}{N} \sum_{j=1}^{N} \frac{1}{d_j} = (N-1)^2 E\left[\frac{1}{D}\right], \tag{B12}$$

which is sharper than the bound $R_G \geqslant \frac{(N-1)^2}{E[D]}$ in Ref. [2, Eq. (7.25) on p. 207], since the harmonic mean of the degree $E[\frac{1}{D}] \geqslant \frac{1}{E[D]}$. The inequality (B11) is further used in Ref. [51] to determine the Kemeny constant, defined by $\frac{d^T \Omega d}{4L}$, where d is the degree vector of the graph G. While the geometric inequality (B11) leads to a new sharp bound (B12), the arithmetic mean companion (B10) leads, after summing over all j in an unweighted graph where $\sum_{j=1}^{N} Q_{jj} = \sum_{j=1}^{N} d_j = 2L$ and $\sum_{j=1}^{N} (\widehat{Q}^{-1})_{ii} = \frac{R_G}{N}$, to

$$L + \alpha \frac{R_G}{2N} \geqslant \sqrt{\alpha}(N-1),$$

which is considerably weaker than (B12).

Theorem 6. Let $\widehat{Q}^{-1}$ denote the pseudoinverse of the unweighted Laplacian Q, and then the diagonal element $(\widehat{Q}^{-1})_{ii}$ is upper bounded by

$$(\widehat{Q}^{-1})_{ii} \leqslant \frac{1}{d_i}\left(1-\frac{1}{N}\right) + \max_{k \neq i} (\widehat{Q}^{-1})_{ki}, \tag{B13}$$

where $\max_{k\neq i} (\widehat{Q}^{-1})_{ki}$ is the second-largest element on row i of the pseudoinverse $\widehat{Q}^{-1}$.

Proof. Yet another representation for $Q^{\dagger}_{jj}$ is deduced from $\widetilde{Q} Q^{\dagger} = Q^{\dagger} \widetilde{Q} = I - \frac{1}{N} J$, as

$$(\widetilde{Q} Q^{\dagger})_{ij} = (Q^{\dagger} \widetilde{Q})_{ij} = \left(1-\frac{1}{N}\right) 1_{\{i=j\}} - \frac{1}{N} 1_{\{i \neq j\}},$$

where we write

$$(\widetilde{Q} Q^{\dagger})_{ij} = \sum_{k=1}^{N} \widetilde{Q}_{ik} Q^{\dagger}_{kj} = \widetilde{Q}_{ii} Q^{\dagger}_{ij} + \sum_{k=1;k\neq i}^{N} \widetilde{Q}_{ik} Q^{\dagger}_{kj}.$$

If $i = j$, then we have

$$\widetilde{Q}_{ii} Q^{\dagger}_{ii} = \left(1-\frac{1}{N}\right) - \sum_{k=1;k\neq i}^{N} \widetilde{Q}_{ik} Q^{\dagger}_{ki} = \left(1-\frac{1}{N}\right) + \sum_{k=1;k\neq i}^{N} \widetilde{A}_{ik} Q^{\dagger}_{ki},$$

which reduces in a unweighted graph to

$$(\widehat{Q}^{-1})_{ii} = \frac{1}{d_i}\left(1-\frac{1}{N}\right) + \frac{1}{d_i} \sum_{k=1;k\neq i}^{N} a_{ik} (\widehat{Q}^{-1})_{ki}. \tag{B14}$$

Using $\min_{k\neq i} (\widehat{Q}^{-1})_{ki} \leqslant \frac{1}{d_i} \sum_{k=1;k\neq i}^{N} a_{ik} (\widehat{Q}^{-1})_{ki} \leqslant \max_{k\neq i} (\widehat{Q}^{-1})_{ki}$, we deduce the lower and upper bound

$$\min_{k\neq i} (\widehat{Q}^{-1})_{ki} \leqslant \left\{ (\widehat{Q}^{-1})_{ii} - \frac{1}{d_i}\left(1-\frac{1}{N}\right) \right\} \leqslant \max_{k\neq i} (\widehat{Q}^{-1})_{ki},$$

leading to (B13). ■

From $Q^{\dagger} u = 0$, which is equivalent to $\sum_{k=1;k\neq i}^{N} Q^{\dagger}_{ki} = -Q^{\dagger}_{ii} \leqslant 0$, we know that $\min_{k\neq i} Q^{\dagger}_{ki} \leqslant \frac{-Q^{\dagger}_{ii}}{N-1} \leqslant 0$ is nonpositive, but $\max_{k\neq i} Q^{\dagger}_{ki} \geqslant \frac{-Q^{\dagger}_{ii}}{N-1}$ could be positive. Hence, the upper bound (B13) is the more interesting bound,

$$0 \leqslant (\widehat{Q}^{-1})_{ii} - \max_{k\neq i} (\widehat{Q}^{-1})_{ki} \leqslant \frac{1}{d_i}\left(1-\frac{1}{N}\right) < \frac{1}{d_i},$$

which tells us that the difference between the diagonal element (which is the largest) and the second largest element on the row i associated with node i is upper bounded by $\frac{1}{d_i}$: the larger the degree, the smaller the gap between the diagonal element $(\widehat{Q}^{-1})_{ii}$ and the second largest element $\max_{k\neq i} (\widehat{Q}^{-1})_{ki}$.

Combining both lower bound (B11) and upper bound (B13) yields

$$\frac{1}{d_i}\left(1-\frac{1}{N}\right)^2 \leqslant (\widehat{Q}^{-1})_{ii} \leqslant \frac{1}{d_i}\left(1-\frac{1}{N}\right) + \max_{k\neq i}(\widehat{Q}^{-1})_{ki}.$$

Thus, if the pseudoinverse $\widehat{Q}^{-1}$ is also a weighted Laplacian, implying that $\max_{k\neq i}(\widehat{Q}^{-1})_{ki} \leqslant 0$ for each node i, then we arrive at

$$\frac{1}{d_i}\left(1-\frac{1}{N}\right)^2 \leqslant (\widehat{Q}^{-1})_{ii} \leqslant \frac{1}{d_i}\left(1-\frac{1}{N}\right).$$

In summary, if the pseudoinverse $\widehat{Q}^{-1}$ of a graph G with N nodes is a weighted Laplacian, then for large N, we find that $(\widehat{Q}^{-1})_{ii} \to \frac{1}{d_i}$ for any node i and that the corresponding ζ vector in (8) tends to $(\frac{1}{d_1}, \frac{1}{d_2}, \ldots, \frac{1}{d_N})$.

Theorem 6 also underlines the importance of the second largest row i element, $\max_{k\neq i}(\widehat{Q}^{-1})_{ki}$. Combining (B14) and (B11) yields

$$\sum_{k=1;k\neq i}^{N} a_{ik}(\widehat{Q}^{-1})_{ki} \geqslant -\left(1-\frac{1}{N}\right)\frac{1}{N}$$

and from $\frac{1}{d_i}\sum_{k=1;k\neq i}^{N} a_{ik}(\widehat{Q}^{-1})_{ki} \leqslant \max_{k\neq i}(\widehat{Q}^{-1})_{ki}$, we obtain

$$\max_{k\neq i}(\widehat{Q}^{-1})_{ki} \geqslant -\left(1-\frac{1}{N}\right)\frac{1}{Nd_i}, \tag{B15}$$

illustrating that $\max_{k\neq i}(\widehat{Q}^{-1})_{ki} \geqslant 0$ tends to be non-negative in any graph with large size N. If equality in this lower bound (B15) can be attained, then the lowest possible upper bound follows from (B13) as

$$(\widehat{Q}^{-1})_{ii} \leqslant \frac{1}{d_i}\left(1-\frac{1}{N}\right)^2,$$

while the lower bound (B11) then indicates that equality must hold

$$(\widehat{Q}^{-1})_{ii} = \frac{1}{d_i}\left(1-\frac{1}{N}\right)^2.$$

Hence, if $\max_{k\neq i}(\widehat{Q}^{-1})_{ki} = -(1-\frac{1}{N})\frac{1}{Nd_i}$ equals its minimum value, then $(\widehat{Q}^{-1})_{ii} = \frac{1}{d_i}(1-\frac{1}{N})^2$, which also is the minimum value.

Let $\widetilde{H}_{ij}$ denote the weight of the shortest path $\mathcal{P}^*_{ij}$ from node i to node j, which equals $\widetilde{H}_{ij} = \sum_{l\in\mathcal{P}^*_{ij}} \frac{1}{r_l}$. Clearly, in an unweighted graph with $r_l = 1$, the matrix $\widetilde{H}$ reduces to the hopcount or distance matrix H, where H_{ij} equals the number of hops or links in the shortest path $\mathcal{P}^*_{ij}$. In general [4], the inequality $\omega_{ij} \leqslant \widetilde{H}_{ij}$ holds. Indeed, equality occurs in a tree, because there is only one shortest path and the inequality arises from the fact that adding links can only decrease the effective graph resistance, because there can be more than one path between i and j and a flow traverses over all possible paths. Hence, an upper bound follows from (B2) as

$$Q^{\dagger}_{ij} \leqslant \frac{u^T\widetilde{H}}{2N}(e_i+e_j) - \frac{\widetilde{R}_G}{N^2}.$$

APPENDIX C: EXPLICIT COMPUTATIONS OF THE PSEUDOINVERSE $Q^{\dagger}$ IN SPECIAL GRAPHS

We derive the pseudoinverse $Q^{\dagger}$ for three special type of graphs: the complete bipartite graph $K_{m,n}$ on $N = n+m$ nodes, the path graph P_N, and the cycle C_N. We assume constant resistances on the link weights, but for the path graph, we also give the complete general case where each link k has a resistance r_k. Expressions for the path and cycle in this section have been determined earlier by Bendito *et al.* [21], using a different method, namely operator calculus.

1. Pseudoinverse of the Laplacian of a complete bipartite graph

The Laplacian of the complete bipartite graph $K_{m,n}$, with total number of nodes $N = n+m$, is [2, p. 130]

$$Q_{K_{m,n}} = \begin{bmatrix} nI_{m\times m} & -J_{m\times n} \\ -J_{n\times m} & mI_{n\times n} \end{bmatrix}.$$

Theorem 7. The pseudoinverse matrix of the Laplacian $Q_{K_{m,n}}$ of a complete bipartite graph $K_{m,n}$ with $N = n+m$ nodes is

$$Q^{\dagger}_{K_{m,n}} = \frac{1}{N^2}\begin{bmatrix} \frac{1}{n}((n+m)^2 I_{m\times m} - (2n+m)J_{m\times m}) & -J_{m\times n} \\ -J_{n\times m} & \frac{1}{m}((n+m)^2 I_{n\times n} - (2m+n)J_{n\times n}) \end{bmatrix}. \tag{C1}$$

Proof. The expression (12) for $\alpha = 1$ of the pseudoinverse of the Laplacian Q suggests us to compute

$$(Q_{K_{m,n}} + J)^{-1} = \begin{bmatrix} nI_{m\times m} + J_{m\times m} & O_{m\times n} \\ O_{n\times m} & mI_{n\times n} + J_{n\times n} \end{bmatrix}^{-1} = \begin{bmatrix} (nI_{m\times m} + J_{m\times m})^{-1} & O_{m\times n} \\ O_{n\times m} & (mI_{n\times n} + J_{n\times n})^{-1} \end{bmatrix}.$$

The inverse of a "rank one update" can be deduced from the Sherman-Morrison-Woodbury formula as

$$(A + cd^T)^{-1} = A^{-1} - \frac{A^{-1}cd^TA^{-1}}{1 + d^TA^{-1}c}. \tag{C2}$$

Since $J_{m\times m} = u_m.u_m^T$, where u_m denotes the $(m\times 1)$ all-one vector, applying the above expression yields

$$(nI_{m\times m} + J_{m\times m})^{-1} = \frac{1}{n}\left(I_{m\times m} - \frac{1}{n+m}J_{m\times m}\right)$$

so that

$$(Q_{K_{m,n}}+J)^{-1}=\begin{bmatrix}\frac{1}{n}\left(I_{m\times m}-\frac{1}{n+m}J_{m\times m}\right) & O_{m\times n}\\ O_{n\times m} & \frac{1}{m}\left(I_{n\times n}-\frac{1}{n+m}J_{n\times n}\right)\end{bmatrix}.$$

The pseudoinverse (12) of the Laplacian Q of the complete bipartite graph $K_{m,n}$ is

$$\begin{aligned}Q^{\dagger}&=\begin{bmatrix}\frac{1}{n}\left(I_{m\times m}-\frac{1}{n+m}J_{m\times m}\right) & O_{m\times n}\\ O_{n\times m} & \frac{1}{m}\left(I_{n\times n}-\frac{1}{n+m}J_{n\times n}\right)\end{bmatrix}\begin{bmatrix}I_{m\times m}-\frac{1}{n+m}J_{m\times m} & -\frac{1}{n+m}J_{m\times n}\\ -\frac{1}{n+m}J_{n\times m} & \left(I_{n\times n}-\frac{1}{n+m}J_{n\times n}\right)\end{bmatrix}\\ &=\begin{bmatrix}\frac{1}{n}\left(I_{m\times m}-\frac{1}{n+m}J_{m\times m}\right)^2 & -\frac{1}{n+m}\frac{1}{n}\left(I_{m\times m}-\frac{1}{n+m}J_{m\times m}\right)J_{m\times n}\\ -\frac{1}{n+m}\frac{1}{m}\left(I_{n\times n}-\frac{1}{n+m}J_{n\times n}\right)J_{n\times m} & \frac{1}{m}\left(I_{n\times n}-\frac{1}{n+m}J_{n\times n}\right)^2\end{bmatrix}.\end{aligned}$$

With $\left(I_{m\times m}-\frac{1}{n+m}J_{m\times m}\right)^2=I_{m\times m}-\frac{2n+m}{(n+m)^2}J_{m\times m}$ and $(I_{m\times m}-\frac{1}{n+m}J_{m\times m})J_{m\times n}=\frac{n}{n+m}J_{m\times n}$, we finally arrive at (C1). ■

The pseudoinverse $Q^{\dagger}$ of the Laplacian almost equals the Laplacian $Q_{K_{m,n}}$, except that the diagonal block matrices are different. The star graph $K_{1,n}$ on $N=n+1$ nodes possesses the pseudoinverse of the Laplacian,

$$Q^{\dagger}_{\text{star}}=\frac{1}{N^2}\begin{bmatrix}n & -J_{1\times n}\\ -J_{n\times 1} & (n+1)^2I_{n\times n}-(2+n)J_{n\times n}\end{bmatrix}.$$

2. Pseudoinverse of the Laplacian of a path graph

a. Algebraic solution

For a path graph with equal link weights b, the Laplacian $\widetilde{Q}$ can be written (see Ref. [2, p. 125]) as

$$\widetilde{Q}=\begin{bmatrix}b & -b & 0 & \dots & 0 & 0\\ -b & 2b & -b & 0 & \dots & 0\\ 0 & \ddots & \ddots & \ddots & & \vdots\\ \vdots & & \ddots & \ddots & \ddots & 0\\ 0 & \dots & 0 & -b & 2b & -b\\ 0 & 0 & \dots & 0 & -b & b\end{bmatrix}=bQ_P.$$

The positive eigenvalues μ_k of the weighted Laplacian $\widetilde{Q}$ of the path graph [2, pp. 126–128] are

$$(\widetilde{\mu}_P)_{N-k}=2b\left[1-\cos\left(\frac{\pi k}{N}\right)\right]=4b\sin^2\left(\frac{\pi k}{2N}\right),$$

where $1\leqslant k\leqslant N-1$ [and $\mu_0=(\widetilde{\mu}_P)_N=0$]. The normalized eigenvector elements of the Laplacian Q of the path graph, corresponding to $\mu_k=(\widetilde{\mu}_P)_{N-k}$, are known as

$$(z_k)_v=\frac{\sqrt{2}}{\sqrt{N}}\cos\left(\frac{\pi kv}{N}-\frac{\pi k}{2N}\right),$$

where $1\leqslant v\leqslant N$ points towards node v in the path graph. The elements of the pseudoinverse of the path graph Laplacian follow from (11) as

$$\begin{aligned}Q^{\dagger}_{ij}&=\sum_{k=1}^{N-1}\frac{(z_k)_i(z_k)_j}{\mu_k}\\ &=\frac{1}{Nb}\sum_{k=1}^{N-1}\frac{\cos\left(\frac{\pi ki}{N}-\frac{\pi k}{2N}\right)\cos\left(\frac{\pi kj}{N}-\frac{\pi k}{2N}\right)}{1-\cos\left(\frac{\pi k}{N}\right)}\\ &=\frac{1}{2Nb}\sum_{k=1}^{N-1}\frac{\cos\left[\frac{\pi k(i+j-1)}{N}\right]+\cos\left[\frac{\pi k(i-j)}{N}\right]}{1-\cos\left(\frac{\pi k}{N}\right)}.\end{aligned}$$

Theorem 8. If we define the trigonometric sum

$$q_N(m)=\sum_{k=1}^{N-1}\frac{\cos\left(\frac{\pi km}{N}\right)}{1-\cos\left(\frac{\pi k}{N}\right)}=\frac{1}{2}\sum_{k=1}^{N-1}\frac{\cos\left(\frac{\pi km}{N}\right)}{\sin^2\left(\frac{\pi k}{2N}\right)},\tag{C3}$$

which is an even function in m, i.e., $q_N(m)=q_N(-m)$ and equal, for $0\leqslant m\leqslant 2N$, to

$$\begin{aligned}q_N(m)=\frac{m^2}{2}-m\left(N+\frac{1}{2}\right)+\frac{(2m+1)+(-1)^{m+1}}{4}\\ +\frac{N^2-1}{3},\end{aligned}\tag{C4}$$

then we can compactly express each element (i,j) of the symmetric pseudoinverse matrix $Q^{\dagger}_{\text{path}}$ of the path graph as

$$(Q_{\text{path}})^{\dagger}_{ij}=\frac{1}{2Nb}\{q_N(i+j-1)+q_N(i-j)\}.\tag{C5}$$

In fact, (C5) shows that the symmetric pseudoinverse matrix $Q^{\dagger}$ is the sum of two symmetric matrices Q_1 and Q_2, where all elements in Q_1 along parallels of the antidiagonal are the same, whereas all elements in Q_2 along parallels of the diagonal are the same. Since $\cos\left[\frac{\pi k}{N}(m+2jN)\right)=\cos\left(\frac{\pi k}{N}m+2\pi kj\right)]=\cos\left(\frac{\pi k}{N}m\right)$ for any integer j, we find periodicity in N,

$$q_N(m)=q_N(m+2jN).$$

Invoking (C19), we have

$$q_N(0)=\frac{1}{2}\sum_{k=1}^{N-1}\frac{1}{\sin^2\left(\frac{\pi k}{2N}\right)}=\frac{N^2-1}{3},\tag{C6}$$

which is the maximum value of $q_N(m)$, because $|q_N(m)|\leqslant\frac{1}{2}\sum_{k=1}^{N-1}\frac{|\cos\left(\frac{\pi km}{N}\right)|}{\sin^2\left(\frac{\pi k}{2N}\right)}\leqslant\frac{1}{2}\sum_{k=1}^{N-1}\frac{1}{\sin^2\left(\frac{\pi k}{2N}\right)}=q_N(0)$.

Proof of Theorem 8. The trigonometric sum $q_N(m)$ in (C3) is evaluating by first deriving a difference equation for $q_N(m)$, which is then solved.

(a) Difference equation for $q_N(m)$. Using

$$\cos\left(\frac{\pi km}{N}\right) - \cos\left(\frac{\pi k(m-1)}{N}\right) = -2\sin\left(\frac{\pi km}{N} - \frac{\pi k}{2N}\right)\sin\left(\frac{\pi k}{2N}\right),$$

the difference $\Delta q_N(m) = q_N(m) - q_N(m-1)$ is

$$\Delta q_N(m) = \frac{1}{2}\sum_{k=1}^{N-1}\frac{\cos\left(\frac{\pi km}{N}\right) - \cos\left[\frac{\pi k(m-1)}{N}\right]}{\sin^2\left(\frac{\pi k}{2N}\right)} = -\sum_{k=1}^{N-1}\frac{\sin\left(\frac{\pi km}{N} - \frac{\pi k}{2N}\right)}{\sin\left(\frac{\pi k}{2N}\right)},$$

from which we find that $\Delta q_N(m)|_{m=0} = q_N(0) - q_N(-1) = q_N(0) - q_N(1) = N-1$. Observing that

$$\sin\left(\frac{\pi k(m+1)}{N} - \frac{\pi k}{2N}\right) - \sin\left(\frac{\pi km}{N} - \frac{\pi k}{2N}\right) = 2\sin\left(\frac{\pi k}{2N}\right)\cos\left(\frac{\pi km}{N}\right),$$

the second-order difference $\Delta^2 q_N(m+1) = \Delta q_N(m+1) - \Delta q_N(m) = q_N(m+1) - 2q_N(m) + q_N(m-1)$ is

$$\Delta^2 q_N(m+1) = -\sum_{k=1}^{N-1}\frac{\sin\left[\frac{\pi k(m+1)}{N} - \frac{\pi k}{2N}\right] - \sin\left(\frac{\pi km}{N} - \frac{\pi k}{2N}\right)}{\sin\left(\frac{\pi k}{2N}\right)} = -2\sum_{k=1}^{N-1}\cos\left(\frac{\pi km}{N}\right).$$

With (C17), we obtain, for $m \neq 0$,

$$\Delta^2 q_N(m+1) = -2\frac{(-1)^{m-1} - 1}{2} = 1 - (-1)^{m-1},$$

while, for $m = 0$,

$$\Delta^2 q_N(m+1)|_{m=0} = -2(N-1).$$

The second-order difference $\Delta^2 q_N(m+1)$ is equivalent to the difference equation, for $m \neq 0$,

$$q_N(m+1) - 2q_N(m) + q_N(m-1) = 1 + (-1)^m \quad \text{(C7)}$$

and, for $m = 0$,

$$q_N(1) - 2q_N(0) + q_N(-1) = 2[q_N(1) - q_N(0)] = -2(N-1). \quad \text{(C8)}$$

(b) Solving the difference equation (C7) for $q_N(m)$. The general solution of the difference equation $q_N(m+1) - 2q_N(m) + q_N(m-1) = f(m)$ for integers $m \neq 0$ and an arbitrary function of $f(m)$ can be deduced with generating functions,

$$T(z) = \sum_{m=0}^{\infty} q_N(m) z^m. \quad \text{(C9)}$$

After multiplying both sides by z^m and summing over all $m > 0$, the difference equation becomes

$$\sum_{m=1}^{\infty} q_N(m+1)z^m - 2\sum_{m=1}^{\infty} q_N(m)z^m + \sum_{m=1}^{\infty} q_N(m-1)z^m = \sum_{m=1}^{\infty} f(m)z^m$$

Written in terms of $F(z) = \sum_{m=0}^{\infty} f(m)z^m$ and $T(z)$,

$$\left(\frac{1}{z} - 2 + z\right)T(z) = F(z) + \{q_N(1) - f(0) - 2q_N(0)\} + \frac{q_N(0)}{z}.$$

Invoking the conditions (C8) and $q_N(0) - (N-1) = q_N(1)$ yields

$$T(z) = \frac{z}{(1-z)^2}F(z) - \{(N-1) + q_N(0) + f(0)\} \times \frac{z}{(1-z)^2} + \frac{q_N(0)}{(1-z)^2}.$$

After expanding the Taylor series around $z = 0$ and using the Cauchy product $\sum_{m=0}^{\infty} f_m z^m \sum_{m=0}^{\infty} g_m z^m = \sum_{m=0}^{\infty}(\sum_{k=0}^{m} f_{m-k}g_k)z^m$, we obtain

$$T(z) = \sum_{m=0}^{\infty}\left\{\sum_{k=0}^{m} kf(m-k) - m\{(N-1) + q_N(0) + f(0)\} + q_N(0)(m+1)\right\}z^m,$$

where we have used the derivative of the geometric series, $\frac{d}{dz}\frac{1}{1-z} = \frac{1}{(1-z)^2} = \sum_{m=1}^{\infty} mz^{m-1}$. Equating corresponding powers in z yields the general solution as a function of $f(m)$ and the initial conditions $q_N(0)$,

$$q_N(m) = \sum_{k=0}^{m} kf(m-k) - m\{(N-1) + f(0)\} + q_N(0). \quad \text{(C10)}$$

For the specific case of $f(m) = 1 + (-1)^m$, the sum in the general solution (C10) becomes

$$\sum_{k=0}^{m} kf(m-k) = \sum_{k=0}^{m} k[1 + (-1)^{k-m}] = \frac{m(m+1)}{2} + \frac{(2m+1) + (-1)^{m+1}}{4},$$

so that (C10) reduces to

$$q_N(m) = \frac{m(m+1)}{2} - m(N+1) + \frac{(2m+1) + (-1)^{m+1}}{4} + q_N(0).$$

Finally, with (C6), we arrive at (C4), for $0 \leqslant m \leqslant 2N$ due to periodicity and $q_N(-m) = q_N(m)$. ■

b. Electrical solution

We compute the nodal voltages in a path graph under a uniform external current $x = e_j - \frac{u}{N}$. The node indexed as 1 is at an end of the path and the resistance between node k and $k+1$ is r_k. For a tree, the effective resistance between any pair of nodes equals the weighted path length between those nodes, see, for example, Refs. [4,13]. The effective resistance between node i and j in the path graph equals $\omega_{ij} = \sum_{k=i}^{j-1} r_k$, for $i < j$, and simplifies for unit resistances, where $r_i = 1$ for all links, to $\omega_{ij} = |i - j|$. Using $J = uu^T$, we rewrite (14) as

$$v = \frac{1}{2}\left(\frac{uu^T}{N} - I\right)\Omega x.$$

Filling in the external current $x = e_j - \frac{u}{N}$ gives

$$\begin{aligned} v &= \frac{1}{2N}\left(\frac{uu^T}{N} - I\right)\Omega(Ne_j - u) \\ &= \frac{1}{2N}\left[u(u^T\Omega e_j) - \frac{1}{N}u(u^T\Omega u) - N\Omega e_j + \Omega u\right] \end{aligned} \quad \text{(C11)}$$

and the ith component of the voltage vector v is

$$v_i = \frac{1}{2N}\left(u^T\Omega e_j - \frac{1}{N}u^T\Omega u - N\omega_{ij} + e_i^T\Omega u\right). \quad \text{(C12)}$$

We calculate the four terms in expression (C12) for v_i using $\omega_{ab} = \sum_{k=a}^{b-1} r_k$ for $a < b$. First, we have

$$\begin{aligned} u^T\Omega e_j &= \sum_{i=1}^{N}\omega_{ij} = \sum_{i=1}^{j}\sum_{k=i}^{j-1} r_k + \sum_{i=j+1}^{N}\sum_{k=j}^{i-1} r_k \\ &= \sum_{k=1}^{j-1} k r_k + \sum_{k=j}^{N-1}(N-k)r_k. \end{aligned}$$

Second,

$$\begin{aligned} \frac{1}{N}u^T\Omega u &= \frac{1}{N}\sum_{i=1}^{N}\sum_{k=1}^{N}\omega_{ik} = \frac{2}{N}\sum_{i=1}^{N}\left(\sum_{j=1}^{i}\sum_{k=j}^{i-1} r_k\right) \\ &= \frac{2}{N}\sum_{i=1}^{N}\sum_{k=1}^{i-1} k r_k = \frac{2}{N}\sum_{k=1}^{N-1} k(N-k)r_k. \end{aligned}$$

Third,

$$e_i^T\Omega u = u^T\Omega e_i = \sum_{k=1}^{i-1} k r_k + \sum_{k=i}^{N-1}(N-k)r_k.$$

Substituting these terms in (C12) and solving for $i \leqslant j$ specifically gives

$$\begin{aligned} v_i &= \frac{1}{2N}\left(u^T\Omega e_j - \frac{1}{N}u^T\Omega u - N\omega_{ij} + u^T\Omega e_i\right) \\ &= \frac{1}{2N}\left[\sum_{k=1}^{j-1} k r_k + \sum_{k=j}^{N-1}(N-k)r_k - \frac{2}{N}\sum_{k=1}^{N-1} k(N-k)r_k \right. \\ &\quad \left. - N\sum_{k=i}^{j-1} r_k + \sum_{k=1}^{i-1} k r_k + \sum_{k=i}^{N-1}(N-k)r_k\right] \\ &= \frac{1}{2N}\left[\sum_{k=1}^{N-1} 2k^2/N r_k + \sum_{k=j}^{N-1} 2(N-k)r_k - \sum_{k=i}^{j-1} 2k r_k\right] \\ &= \frac{1}{N^2}\sum_{k=1}^{N-1} k^2 r_k + \frac{1}{N}\sum_{k=j}^{N-1}(N-k)r_k - \frac{1}{N}\sum_{k=i}^{j-1} k r_k. \end{aligned}$$

After a similar computation for $i > j$, we arrive at the nodal voltage for general resistances r_k,

$$v_i = Q^{\dagger}_{ij} = \begin{cases} \frac{1}{N^2}\sum_{k=1}^{N-1} k^2 r_k + \frac{1}{N}\sum_{k=j}^{N-1}(N-k)r_k - \frac{1}{N}\sum_{k=i}^{j-1} k r_k & \text{if } i \leqslant j \\ \frac{1}{N^2}\sum_{k=1}^{N-1} k^2 r_k + \frac{1}{N}\sum_{k=i}^{N-1}(N-k)r_k - \frac{1}{N}\sum_{k=j}^{j-1} k r_k & \text{if } i > j \end{cases}. \quad \text{(C13)}$$

For unit resistances [$r_k = 1$ for all k in (C13)], we find

$$v_i = -\frac{N^2-1}{6N} + \frac{(N-i)(N-i+1)}{2N},$$

consistent with (28) and (C5) with $b = 1$.

3. Pseudoinverse of the Laplacian of a cycle

Theorem 9. The element (i,j) of the symmetric pseudoinverse matrix $Q_C^{\dagger}$ of the Laplacian Q_C of a cycle (also called circuit or ring) with N nodes is

$$(Q_C^{\dagger})_{ij} = \frac{1}{N}\left[q_{\frac{N}{2}}(i-j) + \frac{(-1)^{i-j}}{4}\right], \quad \text{(C14)}$$

where $q_N(m)$ is defined in (C3) and (C4).

Proof. The Laplacian eigenvalues of the cycle are [2, p. 123], for $m = 1, \ldots, N$,

$$(\mu_C)_m = 2 - 2\cos\left[\frac{2\pi(m-1)}{N}\right] = 4\sin^2\frac{\pi(m-1)}{N}$$

with

$$r_m = \alpha\left[1, \cos\frac{2\pi(m-1)}{N}, \cos\frac{4\pi(m-1)}{N}, \ldots, \cos\frac{2(N-1)\pi(m-1)}{N}\right]$$

and

$$w_m = \alpha\left[0, \sin\frac{2\pi(m-1)}{N}, \sin\frac{4\pi(m-1)}{N}, \ldots, \sin\frac{2(N-1)\pi(m-1)}{N}\right]$$

are two real, orthogonal eigenvectors belonging to the same real eigenvalue $(\mu_C)_{N-(m-2)} = (\mu_C)_m$, with normalization α. In the sequel, we separate between even and odd number of nodes N.

(a) N is even. It follows from (11) that, if N is even,

$$(Q_C^\dagger)_{ij} = \sum_{m=2}^{[\frac{N}{2}]} \frac{(r_m)_i (r_m)_j}{(\mu_C)_m} + \frac{\left(r_{[\frac{N}{2}+1]}\right)_i \left(r_{[\frac{N}{2}+1]}\right)_j}{(\mu_C)_{[\frac{N}{2}+1]}} + \sum_{m=[\frac{N}{2}+2]}^{N} \frac{(w_m)_i (w_m)_j}{(\mu_C)_m}$$

$$= \frac{2}{N}\left[\sum_{m=2}^{[\frac{N}{2}]} \frac{\cos\frac{2\pi i(m-1)}{N}\cos\frac{2\pi j(m-1)}{N} + \sin\frac{2\pi i(m-1)}{N}\sin\frac{2\pi j(m-1)}{N}}{4\sin^2\frac{\pi(m-1)}{N}} + \frac{\cos(\pi i)\cos(\pi j)}{8}\right]$$

and

$$(Q_C^\dagger)_{ij} = \frac{1}{2N}\left\{\sum_{m=1}^{[\frac{N}{2}-1]} \frac{\cos\frac{2\pi(i-j)m}{N}}{\sin^2\frac{\pi m}{N}} + \frac{\cos[\pi(i-j)]}{2}\right\},$$

which we can rewrite in terms of $q_N(m)$ defined in (C3) leading to (C14).

(b) N is odd. If N is odd, then (11) becomes

$$(Q_C^\dagger)_{ij} = \sum_{k=1}^{N-1} \frac{(z_k)_i (z_k)_j}{\mu_k} = \sum_{m=2}^{[\frac{N+1}{2}]} \frac{(r_m)_i (r_m)_j}{(\mu_C)_m} + \sum_{m=[\frac{N+3}{2}]}^{N} \frac{(w_m)_i (w_m)_j}{(\mu_C)_m}$$

$$= \frac{2}{N}\sum_{m=2}^{[\frac{N+1}{2}]} \frac{\cos\frac{2\pi i(m-1)}{N}\cos\frac{2\pi j(m-1)}{N} + \sin\frac{2\pi i(m-1)}{N}\sin\frac{2\pi j(m-1)}{N}}{4\sin^2\frac{\pi(m-1)}{N}}$$

and

$$(Q_C^\dagger)_{ij} = \frac{1}{2N}\sum_{m=2}^{[\frac{N+1}{2}]} \frac{\cos\frac{2\pi(i-j)(m-1)}{N}}{\sin^2\frac{\pi(m-1)}{N}} = \frac{1}{2N}\sum_{m=1}^{[\frac{N-1}{2}]} \frac{\cos\frac{2\pi(i-j)m}{N}}{\sin^2\frac{\pi m}{N}} \stackrel{def}{=} \frac{1}{N}[q_N^*(m)].$$

We mimic some steps in proofs of Theorem 8 to find the difference equation for $q_N^*(m)$. Observing that $q_N^*(m+1) - 2q_N^*(m) + q_N^*(m-1) = -(N-1)$ results in the general solution for $q_N^*(m)$

$$q_N^*(m) = \sum_{k=0}^{m} k f(m-k) - m\left\{\frac{(N-1)}{2} + f(0)\right\} + q_N^*(0), \tag{C15}$$

where $q_N^*(0) = \frac{N^2-1}{12}$ and $f(m-k) = f(0) = 1$. Equation (C15) can be reduced to

$$q_N^*(m) = \frac{m(m+1)}{2} - m\frac{(N+1)}{2} + \frac{N^2-1}{12} = q_{\frac{N}{2}}(m) + \frac{(-1)^m}{4},$$

which leads to the same equation (C14) for $(Q_C^\dagger)_{ij}$ as in the N is even case. ■

4. Trigonometric sums

Invoking the known formula due to Euler [52], which follows after taking the real part of the geometric sum $\sum_{k=0}^{n-1} e^{ikx} = \frac{e^{inx}-1}{e^{ix}-1} = e^{\frac{i(n-1)x}{2}}\frac{\sin(\frac{nx}{2})}{\sin(\frac{x}{2})}$,

$$\sum_{k=0}^{n-1}\cos kx = \frac{\sin\left[x\left(n-\frac{1}{2}\right)\right]}{2\sin\left(\frac{x}{2}\right)} + \frac{1}{2} \tag{C16}$$

yields

$$\sum_{v=1}^{N-1}\cos\left(\frac{\pi m}{N}v\right) = \frac{(-1)^{m-1}-1}{2} \tag{C17}$$

for $m \neq 0$ (nor $m = 2kN$), else $\sum_{v=1}^{N-1}\cos(\frac{\pi m}{N}v) = N-1$.

Theorem 10. For any integer $n > 1$, it holds that

$$r(n) = \sum_{v=1}^{n-1}\frac{1}{\sin^2\left(\frac{\pi v}{n}\right)} = \frac{n^2-1}{3} \tag{C18}$$

and

$$h(n) = \sum_{v=1}^{n-1}\frac{1}{\sin^2\left(\frac{\pi v}{2n}\right)} = 2\left(\frac{n^2-1}{3}\right) = 2r(n). \tag{C19}$$

Proof. (a) We will first show that $r(n) = \frac{1}{2}h(n)$. We start from the definition

$$r(n) = \sum_{v=1}^{n-1} \frac{1}{\sin^2\left(\frac{\pi v}{n}\right)} = \sum_{v=1}^{n-1} \frac{1}{4\sin^2\left(\frac{\pi v}{2n}\right)\cos^2\left(\frac{\pi v}{2n}\right)}$$
$$= \frac{1}{4}\sum_{v=1}^{n-1} \frac{1}{\sin^2\left(\frac{\pi v}{2n}\right)} + \frac{1}{4}\sum_{v=1}^{n-1} \frac{1}{\cos^2\left(\frac{\pi v}{2n}\right)}.$$

Let $k = n - v$ in the last sum, then

$$\sum_{v=1}^{n-1} \frac{1}{\cos^2\left(\frac{\pi v}{2n}\right)} = \sum_{k=1}^{n-1} \frac{1}{\cos^2\left(\frac{\pi}{2n}(n-k)\right)} = \sum_{k=1}^{n-1} \frac{1}{\sin^2\left(\frac{\pi}{2n}k\right)}.$$

Combined, it yields

$$r(n) = \frac{1}{2}\sum_{v=1}^{n-1} \frac{1}{\sin^2\left(\frac{\pi v}{2n}\right)} = \frac{1}{2}h(n).$$

Since the equality (C19) directly follows from the truth of equality (C18), it remains to demonstrate the equality (C18) for $r(n)$.

(b) Consider

$$r(2n) = \sum_{v=1}^{2n-1} \frac{1}{\sin^2\left(\frac{\pi v}{2n}\right)} = \sum_{v=1}^{n-1} \frac{1}{\sin^2\left(\frac{\pi v}{2n}\right)} + \sum_{v=n}^{2n-1} \frac{1}{\sin^2\left(\frac{\pi v}{2n}\right)}.$$

The last sum equals

$$\sum_{v=n}^{2n-1} \frac{1}{\sin^2\left(\frac{\pi v}{2n}\right)} = \sum_{v=0}^{n-1} \frac{1}{\sin^2\left(\frac{\pi v}{2n} + \frac{\pi}{2}\right)} = \sum_{v=0}^{n-1} \frac{1}{\cos^2\left(\frac{\pi v}{2n}\right)}$$
$$= \sum_{v=1}^{n-1} \frac{1}{\cos^2\left(\frac{\pi v}{2n}\right)} + 1.$$

Thus,

$$r(2n) = 1 + \sum_{v=1}^{n-1}\left[\frac{1}{\sin^2\left(\frac{\pi v}{2n}\right)} + \frac{1}{\cos^2\left(\frac{\pi v}{2n}\right)}\right]$$
$$= 1 + \sum_{v=1}^{n-1} \frac{1}{\sin^2\left(\frac{\pi v}{2n}\right)\cos^2\left(\frac{\pi v}{2n}\right)} = 1 + 4\sum_{v=1}^{n-1} \frac{1}{\sin^2\left(\frac{\pi v}{n}\right)}$$

and this relation establishes the recursion

$$r(2n) = 4r(n) + 1. \tag{C20}$$

In addition, $r(2) = \frac{1}{\sin^2(\frac{\pi}{2})} = 1$. A few times iterating (C20) yields

$$r(n) = 4^k r\left(\frac{n}{2^k}\right) + \frac{4^k - 1}{3}.$$

If $n = 2.2^k$, then

$$r(2^k) = (2^k)^2 r\left(\frac{n}{2^k}\right) + \frac{(2^k)^2 - 1}{3}$$
$$= (2^k)^2 r(2) + \frac{(2^k)^2 - 1}{3} = \frac{4(2^k)^2 - 1}{3},$$

which suggests that

$$r(n) = \frac{4(n/2)^2 - 1}{3} = \frac{n^2 - 1}{3}.$$

Indeed, we readily verify that the right-hand side of (C18) satisfies the recursion (C20):

$$\frac{(2n)^2 - 1}{3} = 4\frac{n^2 - 1}{3} + 1 = \frac{(2n)^2 - 4 + 3}{3},$$

which proves (C18). ∎

The second identity in Theorem 10 does not seem to appear in textbooks. The expression $r(n)$ was earlier derived in Ref. [2, p. 207] and Ref. [4], because the effective graph resistance of the path on n nodes equals $R_{(n-1)\text{hop path}} = \frac{(n-1)n(n+1)}{6} = \frac{n}{2}r(n)$.

APPENDIX D: LAPLACIAN PSEUDOINVERSE OF THE COMPLEMENT OF A GRAPH

The adjacency matrix of the complement of a graph is $A^c = J - I - A$: If there is a link between node i and j in G, then there is no link between node i and j in its complement G^c. Thus, the remainder of this section concentrates on unweighted graphs. The Laplacian Q^c of the complement of a graph has [2] the same set of eigenvectors as that of the Laplacian Q. If $Q = \sum_{k=1}^{N-1} \mu_k z_k z_k^T$, then

$$Q^c = \sum_{k=1}^{N-1} (N - \mu_k) z_k z_k^T.$$

Consequently, assuming that both the graph G and its complement G^c are connected, $0 < \mu_{N-1} < \mu_1 < N$, the Laplacian pseudoinverse of the complement of a graph is

$$\left(\widehat{Q^c}\right)^{-1} = \sum_{k=1}^{N-1} \frac{1}{N - \mu_k} z_k z_k^T$$

and, in matrix form,

$$\left(\widehat{Q^c}\right)^{-1} = Z(NI - M)^{-1}Z^T = (\alpha I - Q)^{-1}\big|_{\alpha=N},$$

where $(\alpha I - Q)^{-1}$ is known [2, p. 243] as the resolvent of Q. From (B1), the diagonal element corresponding to node j in Laplacian pseudo-inverse of G^c is

$$\left(\widehat{Q^c}\right)^{-1}_{jj} = \sum_{k=1}^{N-1} \frac{1}{N - \mu_k} (z_k)_j^2$$

and (13) shows that the effective graph resistance of the complement G^c is

$$R_{G^c} = N\sum_{k=1}^{N-1} \frac{1}{N - \mu_k}. \tag{D1}$$

1. The effective graph resistance R_{G^c} of the complement G^c of the graph G

Introducing the Taylor expansion $\frac{1}{N-\mu_k} = \frac{1}{N(1-\frac{\mu_k}{N})} = \sum_{m=0}^{\infty} \mu_k^m \frac{1}{N^{m+1}}$, convergent because of the assumption $\mu_1 < N$, into (D1) yields

$$R_{G^c} = \sum_{m=0}^{\infty} \frac{1}{N^m} \sum_{k=1}^{N-1} \mu_k^m.$$

Since

$$\sum_{k=1}^{N-1}\mu_k^m = \mu_1^m\sum_{k=1}^{N-1}\left(\frac{\mu_k}{\mu_1}\right)^m = \mu_1^m\left[1+\sum_{k=2}^{N-1}\left(\frac{\mu_k}{\mu_1}\right)^m\right] < \mu_1^m\left[1+(N-2)\left(\frac{\mu_2}{\mu_1}\right)^m\right] < \mu_1^m(N-1),$$

the mth term in the series

$$\frac{\sum_{k=1}^{N-1}\mu_k^m}{N^m} < \left(\frac{\mu_1}{N}\right)^m(N-1)$$

decreases exponentially in m because $\frac{\mu_1}{N} < 1$. Moreover, since all terms are positive, we obtain the lower bound

$$R_{G^c} > \sum_{m=0}^{K}\frac{1}{N^m}\sum_{k=1}^{N-1}\mu_k^m$$

for each finite integer K. Using $\sum_{k=1}^{N-1}\mu_k = 2L$, $\sum_{k=1}^{N-1}\mu_k^2 = 2L+\sum_{k=1}^{N}d_k^2$, and $\sum_{k=1}^{N}\mu_k^3 = \sum_{k=1}^{N}d_k^3 + 3\sum_{k=1}^{N}d_k^2 - 6\blacktriangle_G$ as derived in Ref. [2], we obtain

$$\begin{aligned}R_{G^c} &= N-1+\frac{2L}{N}+\frac{2L+\sum_{k=1}^{N}d_k^2}{N^2} + \frac{\sum_{k=1}^{N}d_k^3+3\sum_{k=1}^{N}d_k^2-6\blacktriangle_G}{N^3}+O\left(\frac{\sum_{k=1}^{N-1}\mu_k^4}{N^4}\right)\\ &= N-1+E[D]+\frac{E[D]+E[D^2]}{N} + \frac{E[D^3]+3E[D^2]}{N^2}-\frac{6\blacktriangle_G}{N^3}+(N-1)O\left[\left(\frac{\mu_1}{N}\right)^4\right],\end{aligned}$$

which holds for any pair of connected graphs and complementary graphs and thus excludes the complete graph that attains the minimum possible effective graph resistance $\min_G R_G = N-1$. Thus, for any connected graph G whose complement G^c is also connected, we can write

$$R_G > N-1+E[D^c]+\frac{E[D^c]+E[(D^c)^2]}{N} + \frac{E[(D^c)^3]+3E[(D^c)^2]}{N^2}-\frac{6\blacktriangle_{G^c}}{N^3},$$

where $D^c = N-1-D$ is the degree of a random node in the complementary graph. The smaller the largest Laplacian eigenvalue μ_1, the sharper the lower bound is.

Invoking the harmonic, geometric, and arithmetic mean inequality [53]

$$\frac{n}{\sum_{j=1}^{n}\frac{1}{a_j}} \leqslant \sqrt[n]{\prod_{j=1}^{n}a_j} \leqslant \frac{1}{n}\sum_{j=1}^{n}a_j \tag{D2}$$

yields

$$\frac{N-1}{\sum_{k=1}^{N-1}\frac{N}{\mu_k(N-\mu_k)}} \leqslant \frac{1}{N(N-1)}\sum_{k=1}^{N-1}\mu_k(N-\mu_k) = E[D]-\frac{E[D^2]}{(N-1)}.$$

With

$$\frac{R_{G^c}+R_G}{N} = \sum_{k=1}^{N-1}\frac{N}{\mu_k(N-\mu_k)},$$

we thus find that

$$\frac{N(N-1)}{E[D]-\frac{E[D^2]}{N-1}} \leqslant R_{G^c}+R_G.$$

For a connected ER random graph $G_p(N)$ and its connected complement $G_p^c(N) = G_{1-p}(N)$, the last inequality becomes

$$R_{G_p(N)}+R_{G_{1-p}(N)} \geqslant \frac{N(N-1)}{(N-1)p-(N-2)p^2-p} = \frac{N(N-1)}{(N-2)p(1-p)}$$

or, simplified,

$$R_{G_p(N)}+R_{G_{1-p}(N)} > \frac{N}{p(1-p)}.$$

[1] P. Van Mieghem, Graph eigenvectors, fundamental weights and centrality metrics for nodes in networks, arXiv:1401.4580.

[2] P. Van Mieghem, *Graph Spectra for Complex Networks* (Cambridge University Press, Cambridge, 2011).

[3] D. J. Klein and M. Randić, Resistance distance, J. Math. Chem. **12**, 81 (1993).

[4] W. Ellens, F. A. Spieksma, P. Van Mieghem, A. Jamakovic, and R. E. Kooij, Effective graph resistance, Linear Algebra Appl. **435**, 2491 (2011).

[5] L. Lovász, Random walks on graphs: A survey, Combinatorics **2**, 1–46 (1993).

[6] A. K. Chandra, P. Raghavan, W. L. Ruzzo, and R. Smolensky, The electrical resistance of a graph captures its commute and cover times, in *Proceedings of the 21st Annual ACM Symposium on Theory of Computing (STOC'89)* (ACM, New York, 1989), pp. 574–586.

[7] M. E. J. Newman, A measure of betweenness centrality based on random walks, arXiv:cond-mat/0309045.

[8] Y. Koç, M. Warnier, P. Van Mieghem, R. E. Kooij, and F. M. T. Brazier, The impact of the topology on cascading failures in a power grid model, Physica A (Amsterdam) **402**, 169 (2014).

[9] Y. Koç, M. Warnier, P. Van Mieghem, R. E. Kooij, and F. M. T. Brazier, A topological investigation of phase transitions of cascading failures in power girds, Physica A (Amsterdam) **415**, 273 (2014).

[10] H. Cetinay, F. A. Kuipers, and P. Van Mieghem, A topological investigation of power flow, IEEE Syst. J. (2016), doi: 10.1109/JSYST.2016.2573851.

[11] X. Wang, E. Pournaras, R. E. Kooij, and P. Van Mieghem, Improving robustness of complex networks via the effective graph resistance, Eur. Phys. J. B **87**, 221 (2014).

[12] G. E. Shilov, *Linear Algebra* (Dover Pubications, New York, 1977).

[13] A. Ghosh, S. Boyd, and A. Saberi, Minimizing effective resistance of a graph, SIAM Rev. **50**, 37 (2008).

[14] M. Fiedler, Geometry of the Laplacian, Linear Algebra Appl. **403**, 409 (2005).

[15] G. Ranjan and Z.-L. Zhang, Geometry of complex networks and topological centrality, Physica A (Amsterdam) **392**, 3833 (2013).

[16] P. Van Mieghem, *Performance Analysis of Complex Networks and Systems* (Cambridge University Press, Cambridge, 2014).

[17] P. Van Mieghem, J. Omic, and R. E. Kooij, Virus spread in networks, IEEE/ACM Trans. Netw. **17**, 1 (2009).

[18] P. Van Mieghem and E. Cator, Epidemics in networks with nodal self-infections and the epidemic threshold, Phys. Rev. E **86**, 016116 (2012).

[19] P. G. Doyle and J. L. Snell, Random walks and electric networks, arXiv:math/0001057.

[20] F. Chung and S.-T. Yau, Discrete Green's functions, J. Comb. Theory, Ser. A **91**, 191 (2000).

[21] E. Bendito, A. Carmona, A. M. Encinas, and M. Mitjana, Generalized inverses of symmetric M-matrices, Linear Algebra Appl. **432**, 2438 (2010).

[22] M. Fiedler, Some characterizations of symmetric inverse M-matrices, Linear Algebra Appl. **275-276**, 179 (1998).

[23] C. D. Meyer, *Matrix Analysis and Applied Linear Algebra* (SIAM, Philadelphia, 2000).

[24] H. S. M. Coxeter, The circumradius of the general simplex, Math. Gazette **15**, 229 (1930).

[25] C. J. Stam, E. C. W. van Straaten, E. Van Dellen, P. Tewarie, G. Gong, A. Hillebrand, J. Meier, and P. Van Mieghem, The relation between structural and functional connectivity patterns in complex brain networks, Int. J. Psychophysiol. **103**, 149 (2016).

[26] J. Meier, P. Tewarie, A. Hillebrand, L. Douw, B. W. van Dijk, S. M. Stufflebeam, and P. Van Mieghem, A mapping between structural and functional brain networks, Brain Connect. **6**, 298 (2016).

[27] K. Menger, New foundation of Euclidean geometry, Am. J. Math. **53**, 721 (1931).

[28] G. E. Sharpe, On the $(m+1)$-terminal resistive-network problem, Proc. IEE **116**, 503 (1969).

[29] D. W. Mitchel, 88.27 more on spreads and non-arithmetic means, Math. Gazette **88**, 142 (2004).

[30] S. Boccaletti, V. Latora, Y. Moreno, M. Chavez, and D. Hwang, Complex networks: Structure and dynamics, Phys. Rep. **424**, 175 (2006).

[31] L. Da F. Costa, F. A. Rodrigues, G. Travieso, and P. R. Villas Boas, Characterization of complex networks: A survey of measurements, Adv. Phys. **56**, 167 (2007).

[32] J. Martín Hernández and P. Van Mieghem, Classification of graph metrics, Delft University of Technology, Report20111111, www.nas.ewi.tudelft.nl/people/Piet/TUDelftReports

[33] A. Barrat, M. Bartelemy, and A. Vespignani, *Dynamical Processes on Complex Networks* (Cambridge University Press, Cambridge, 2008).

[34] M. Dehmer and F. Emmert-Streib, *Analysis of Complex Networks* (Wiley-VCH Verlag GmbH& Co., Weinheim, 2009).

[35] M. E. J. Newman, *Networks: An Introduction* (Oxford University Press, Oxford, 2010).

[36] R. Cohen and S. Havlin, *Complex Networks: Structure, Robustness and Function* (Cambridge University Press, Cambridge, 2010).

[37] E. Estrada, *The Structure of Complex Networks* (Oxford University Press, Oxford, 2012).

[38] A. L. Barabási, *Network Science* (Cambridge University Press, Cambridge, 2016).

[39] M. Kitsak, L. K. Gallos, S. Havlin, F. Liljeros, L. Muchnik, H. E. Stanley, and H. A. Makse, Identification of influential spreaders in complex networks, Nat. Phys. **6**, 888 (2010).

[40] F. Morone and H. A. Makse, Influence maximization in complex networks through optimal percolation, Nature **524**, 65 (2015).

[41] D. Kempe, J. Kleinberg, and E. Tardos, Maximizing the spread of influence through a social network, in *Proceedings of the 9th ACM SIGKDD International Conference on Knowledge Discovery and Data Mining* (ACM, New York, 2003), pp. 137–143.

[42] P. Van Mieghem, D. Stevanović, F. A. Kuipers, C. Li, R. van de Bovenkamp, D. Liu, and H. Wang, Decreasing the spectral radius of a graph by link removals, Phys. Rev. E **84**, 016101 (2011).

[43] P. Van Mieghem, H. Wang, X. Ge, S. Tang, and F. A. Kuipers, Influence of assortativity and degree-preserving rewiring on the spectra of networks, Eur. Phys. J. B **76**, 643 (2010).

[44] C. Li, Q. Li, P. Van Mieghem, H. E. Stanley, and H. Wang, Correlation between centrality metrics and their application to the opinion model, Eur. Phys. J. B **88**, 65 (2015).

[45] C. Li, H. Wang, W. de Haan, C. J. Stam, and P. Van Mieghem, The correlation of metrics in complex networks with applications in functional brain networks, J. Stat. Mech. (2011) P11018.

[46] H. Wang, J. Martin Hernandez, and P. Van Mieghem, Betweenness centrality in weighted networks, Phys. Rev. E **77**, 046105 (2008).

[47] J. Martin-Hernandez, Z. Li, and P. Van Mieghem, Weighted betweenness and algebraic connectivity, J. Complex Netw. **2**, 272 (2014).

[48] V. Gurvich, Metric and ultrametric spaces of resistances, Discr. Appl. Math. **158**, 1496 (2010).

[49] P. A. M. Dirac, *The Principles of Quantum Mechanics*, 4th ed. (Clarendon Press, Oxford, 1986).

[50] C. Cohen-Tannoudji, B. Diu, and F. Laloë, *Mécanique Quantique*, Vols. I and II (Hermann, Paris, 1977).

[51] X. Wang, J. L. A. Dubbeldam, and P. Van Mieghem, Kemeny's constant and the effective graph resistance, Linear Algebra Appl. (to be published).

[52] L. Euler, *Introductio in Analysin Infinitorum*, Vol. I (Julius Springer, Berlin, 1748) [German translation by H. Maser in 1885]

[53] G. H. Hardy, J. E. Littlewood, and G. Polya, *Inequalities*, 2nd ed. (Cambridge University Press, Cambridge, UK 1999).